ASSESSING HEAT MITIGATION CAPACITY OF URBAN GREEN SPACES USING THE INVEST MODEL: A SCENARIO ANALYSIS OF SAMANABAD TOWN, LAHORE

Research By

Urva Nadeem 2020-CRP-05

Eliza Naeem 2020-CRP-16

Tooba Iftikhar 2020-CRP-17

Research Supervisor:

Dr. Shaker Mahmood

2020-2024

DEPARTMENT OF CITY AND REGIONAL PLANNING

UNIVERSITY OF ENGINEERING & TECHNOLOGY, LAHORE

ASSESSING HEAT MITIGATION CAPACITY OF URBAN GREEN SPACES USING THE INVEST MODEL: A SCENARIO ANALYSIS OF SAMANABAD TOWN, LAHORE

by

URVA NADEEM, ELIZA NAEEM AND TOOBA IFTIKHAR

A THESIS

presented to the university of engineering and technology, Lahore in partial fulfillment of the requirements for the degree of

Bachelor of Science

in

CITY AND REGIONAL PLANNING

APPROVED BY:

Internal Examiner [Dr. Shaker Mahmood]	External Examiner [Muhammad Tahir]
Chairman of DCRP [Dr. Shaker Mahmood]	Dean of Arch. and Planning [Dr. Rizwan Hameed]

Approval Date

DEPARTMENT OF CITY AND REGIONAL PLANNING
UNIVERSITY OF ENGINEERING & TECHNOLOGY, LAHORE

DECLARATION

It is hereby declared that this research, entitled ‘Assessing Heat Mitigation capacity of Urban Green Spaces Using the InVEST Model: A Scenario Analysis of Samanabad Town, Lahore’ is an original and authentic work of the authors. It is further guaranteed that current work is not submitted for the acquisition of any degree or qualification at any other institute besides University of Engineering & Technology Lahore for the partial fulfilment of BSc. in City and Regional Planning degree requirement. It is assured that; this thesis does not contain any formerly published data except where the references are quoted.

ACKNOWLEDGEMENTS

In the name of ALLAH, the most Beneficent and Merciful who gave us guidance and perseverance to carry out and complete this project, Assessing Heat Mitigation capacity of Urban Green Spaces Using the InVEST Model: A Scenario Analysis of Samanabad Town, Lahore. Our research work would not have been possible without the supervision and assistance of many people. We extend our dearest gratitude for their valuable time and extensive effort in this work.

Our gratitude and appreciation go to our esteemed thesis advisor and mentor Prof. Dr. Shaker Mehmood Mayo for his motivation and support during the course of our studies. Their share of knowledge and counseling made our thesis more interesting and challenging. Our special thanks go to our peers who supported and motivated us throughout the experiment. From their feedback and suggestions, we have learned so much, it is impossible to name those who lent their help and many could be overlooked. In light of the circumstance, we have decided it is best not to name them.

ABSTRACT

Anthropogenic activities have led to profound environmental changes, including melting glaciers, rising sea levels, and intensified heatwaves, posing significant threats to human health, labor productivity, and socioeconomic stability. In response, efforts are underway to mitigate the impacts of global warming and safeguard communities from escalating risks. This study aims to validate the efficacy of the InVEST 3.14.2 Urban Cooling Model (UCM) in characterizing urban thermal environments. The research addresses the need for simplified assessment tools bridging academic expertise with practical applications in urban planning.

Taking Samanabad Town in Lahore as a case study area, the study examines the correlation between cooling capacity (CC) and Land Surface Temperature (LST) imagery at spatial resolutions of 10 and 20 meters. Results demonstrate that higher CC values correspond to lower surface temperatures, with water bodies exhibiting the most significant cooling effect. Variability in LST within different land cover types underscores the heterogeneous nature of surface temperature distributions influenced by factors beyond CC alone.

Recommendations include integrating climatic knowledge into urban planning practices to enhance resilience to extreme heat events and mitigate adverse health impacts. Policy implementation strategies should be refined to address local temperature effects consistently, with a focus on clean green initiatives informed by scientific modeling and research. As spatial data availability improves, there is an opportunity to develop globally applicable approaches for assessing natural infrastructure in urban areas, facilitating informed decision-making and sustainable urban development.

LIST OF CONTENTS

LIST OF FIGURES

LIST OF TABLES

LIST OF ABBREVIATIONS

AOI	Area of Interest
CC	Cooling Capacity
EM	Emissivity
ETI	Evapotranspiration Index
FV	Fraction of Vegetation
GEE	Google Earth Engine
HMI	Heat Mitigation Index
LULC	Land Use and Land Cover
UCM	Urban Cooling Model
UGS	Urban Green Spaces
UHI	Urban Heat Island

1 INTRODUCTION

In today's world, where information is everywhere, the numbers show that global warming is a serious and urgent issue and demands our immediate attention (X. L. Chen et al., 2006; Lima et al., 2021; W. Zhang et al., 2014). This concern has sparked worldwide debate and research into ways to lessen the greenhouse effect and reduce carbon dioxide levels in the atmosphere (Gratani et al., 2016). The present concentrations of worldwide carbon dioxide emissions, according to the Intergovernmental Panel on Climate Change (IPCC), are substantially greater than those predicted by the most pessimistic forecast (IPCC — Intergovernmental Panel on Climate Change, 2023). Melting glaciers, rising sea levels, deadly disease outbreaks, changing rainfall patterns and other social issues are there all because of anthropogenic activities, and now humans are putting efforts to save their communities from potential threats of global warming (Marland et al., 2003).

Under the influence of global warming, there has been an observed escalation in the frequency, intensity, and temporal extent of heatwaves (Luo et al., 2024) during the past decades posing a significant threat to population health (de Bont et al., 2024), labor productivity (Dunne et al., 2013) and socioeconomic costs (Sun et al., 2024). Heatwaves are one of the world's most underestimated threats, killing over 12,000 people annually, making them deadlier than any other weather-related event.

Urbanization, on one hand, is largely advantageous as it leads to improved living standards. Urban areas contribute over 90% of the global gross value added (Phelan et al., 2015), showcasing their significant economic impact and role in driving prosperity and development. On the other side, the very phenomenon has disrupted natural surface energy balances and water cycles in cities, converting vegetated surfaces to heat-retaining impervious surfaces and diminishing urban canopy coverage, leading to increased surface temperatures (Nice et al., 2024). Cities everywhere are hitting record-high summer temperatures (Yin et al., 2024).

Heatwaves are associated with climate warming and extreme weather events, inflamed by rapid urbanization, industrialization, deforestation, CO_2 emissions, mangrove forest degradation, and land use changes (A. Arshad et al., 2020). The dense urban infrastructure has intensified heat accumulation, giving rise to the urban heat island (UHI) effect and

resulting in heterogeneous thermal distributions across different neighborhoods within the city. The issue will only escalate as global temperatures continue to move in their upward trajectory (Rauf et al., 2017).

Urban green spaces (UGS) can play a major role in reducing the heat load caused by built-up areas (Sun et al., 2020). They significantly enhance the environmental quality of cities by improving shading, optimizing landscaping, and increasing evapotranspiration rates (Pauleit et al., 2017). Vegetation play a crucial role in moderating temperatures in urban environments by absorbing and controlling the sun's rays. They contribute to lowering temperatures during the summer and increasing them by 5-8°C on average in open urban spaces compared to areas without trees during winter nights (Onder & Dursun, 2010). Additionally, they contribute to atmospheric purification and carbon sequestration, which collectively result in reduced ambient temperatures and decreased energy consumption (Gallay et al., 2023). Within urban environments, UGS are invaluable assets that promote social interactions, enhance well-being, improve human health, and provide alternative livelihood opportunities (Sirakaya et al., 2018).

Having such significance, these spaces have often been neglected and ignored as they failed to become a main aspect of our city planning and processes. There are numerous challenges to both creating and protecting green spaces amid broader urban development (Practical Considerations and Challenges to Greenspace - Forest Research, 2024). One issue identified is the insufficient presence of UGS in densely populated urban areas and the elimination of existing green spaces during the densification of city areas (Haaland & van den Bosch, 2015). Maintaining UGS incurs costs. Consequently, where green spaces are perceived as deteriorating, there's a heightened risk of redevelopment rather than renovation (Lee et al., 2015). Thus, such green spaces have been converted to grey infrastructure to meet housing needs of the growing population.

Increasing temperatures are frequently documented in Asian nations such as Pakistan, India, Sri Lanka, Afghanistan, and Bangladesh (A. Arshad et al., 2020). Beyond the rising baseline temperatures, uncontrolled urbanization worsens the UHI effect, posing an additional significant threat to these developing countries. Pakistan, with a population of 236 million, has 88 million people residing in urban areas as recorded in 2022 (Pakistan Population (2024) - Worldometer, 2024; Pakistan Urban Population 1960-2024 | MacroTrends, 2024). The rapid

expansion of urban areas of Pakistani cities is beginning to manifest its effects on the local urban climate. S. Arshad et al., 2022 said that urban development in Lahore from 2003 to 2019 has led to a 36% decline in urban vegetation and a 16% increase at the Union Council (UC) level. He further said that areas undergoing development, characterized by sand, vacant, and barren land, typically experience a mean 3-4°C higher LST. We need a better understanding or various urban land uses and their placement to control the overall thermal environment at the city scale.

In this era when artificial intelligence in on continuous rise, studies has been undertaken that utilize deep learning models and advance machine learning to understand and solve complex urban problems. Implications and evolution have been seen in the urban planning tools. For instance, Esri ArcGIS pro has deep learning tools include tree point classification, land cover classification, building footprint extraction and such others (Ready-to-Use Geospatial Deep Learning Models, 2024). These models are part of the ArcGIS Living Atlas of the World and can be used with ArcGIS Pro, ArcGIS Image Server, and ArcGIS API for Python. Similarly, QGIS has several AI extensions, including the Artificial Intelligence Forecasting Remote Sensing (AIRS) plugin, which allows time series forecasting using deep learning models, and the Modzy plugin (Artificial Intelligence Forecasting Remote Sensing — QGIS Python Plugins Repository, 2024).

Humans are considering AI as a potential threat to their species but they need to be focused on saving the most important thing necessary for the survival of all species. That is our Earth. Our planet has been eaten away by the harmful human activities as industrial revolution revolutionized the world by converting breathable land to dead stinking surfaces. All those barren and degraded pieces of land are left abandoned, meanwhile we are out there, seeking for new lands to exploit. Global warming is gone as we are entering in this phase of global boiling.

Developing countries are facing the worst scenarios of climate change. An eye-opening piece of data shared by Dr Hanif was that Lahore is now the most vulnerable city in Pakistan, experiencing climate impacts for 150 days a year (Pakistan: From Global Warming To Global Boiling, 2024). This includes 75 extremely hot days (from May to September), 30 days of smog, 35 days of dense fog, and 10 days of urban flooding. As a result, the people of Lahore endure harsh conditions 40% of the year. Further he added that the UHI effect in

Pakistan has significantly increased, by about 25%, due to the rise of concrete structures and the lack of green spaces.

Practitioners in Pakistan are lacking advanced skills and the system is stagnant and the town planners are no exception. All the research being done in Pakistan is limited to research papers and not being implemented in actual scenarios. Gaining insights into the quantifiable benefits of natural infrastructure, including their distribution and recipients, empowers local governments to make informed investment decisions. Additionally, it provides valuable guidance for private sector entities, non-governmental organizations, civil society groups, and researchers to integrate scientific and technological innovations into on-the-ground projects.

1.1 STATEMENT OF PROBLEM

Urban areas in Pakistan are facing challenges due to increasing temperatures and the UHI effect. Despite this, there's a lack of understanding about how effective strategies like green infrastructure are in Pakistani cities. Also, there's not enough validation of advanced modeling tools in Pakistan.

Previous studies have looked into urban heat mitigation strategies and the UHI effect, but they often don't focus on the specific conditions in Pakistani cities. Also, the lack of validation studies for advanced modeling tools means there's not enough evidence for making decisions about urban environmental management in Pakistan.

This study aims to fill these gaps by validating how well the InVEST UCM represents urban thermal environments in Pakistani cities. By doing this, it aims to make it easier to use advanced modeling tools in real-world urban planning.

This research is crucial for making better decisions about managing urban environments in Pakistan. By validating advanced modeling, it will give us valuable information about how to add the factors of sustainability and resilience in our rapidly urbanizing cities.

1.2 AIMS AND OBJECTIVES

We aim to validate the effectiveness of the InVEST 3.14.2 UCM in representing urban thermal environments. Specifically, we seek to determine whether the Heat Mitigation Index (HMI) generated by the model can serve as an accurate substitute for LST mapping. This

research addresses the need for simplified assessment tools to bridge the gap between academic expertise and practical applications in urban planning departments.

- To validate the representativeness of the HMI in assessing the CC of UGS.
- To examine Samanabad Town of Lahore as a case study area to validate the model and ensure a comprehensive analysis across different urban landscapes.
- To determine the correlation between CC and LST imagery captured on a warm summer day at spatial resolutions of 10 and 20 meters.
- To test the hypothesis that low CC correspond to the highest temperatures in the LST image, and high CC values correspond to the lowest temperatures.
- To estimate the changes in LST due to variations in CC for model outputs.
- To utilize the study for informed urban planning and developing design strategies aimed at enhancing the cooling capacity of UGS.

1.3 SCOPE OF THE STUDY

The study focuses specifically on the urban environment of Samanabad Town and does not extend to other areas of Lahore. It was selected as the case study area due to its representative urban characteristics, presence of water body, inner city open spaces, agricultural fields and it has a manageable size for modeling purposes. Utilizing a smaller case study area allows for efficient simulation runs with the InVEST Urban Cooling Model (UCM), considering the extensive computational resources required for larger urban areas.

July of 2023 was selected as the focal month for data collection and analysis due to its historically highest recorded temperatures, providing a representative snapshot of peak summer conditions in Lahore. Data collected during this period offer insights into the temperature dynamics of the urban environment, crucial for assessing the efficacy of heat mitigation measures and green infrastructure interventions.

The study examines variables related to urban heat mitigation, including LST, vegetation cover, and CC, albedo, precipitation, evapotranspiration, land use and land cover (LULC), UHI, air temperature, building footprint data and shade.

The InVEST 3.14.2 UCM is utilized to simulate urban thermal environments. The central phenomenon of interest is the effectiveness of the model in representing urban thermal environments and assessing the cooling potential of green infrastructure.

The research adopts a quantitative approach, utilizing spatial analysis techniques and model simulations to evaluate the relationship between CC and land surface temperature. The study employs both descriptive and inferential statistical analyses to validate the model outputs and draw conclusions regarding the CC of UGS.

1.4 LIMITATIONS OF STUDY

Despite the comprehensive approach employed in this research, several limitations must be acknowledged to contextualize the interpretation of findings and guide future research. These limitations encompass spatial, temporal, modeling, data availability, interpretational, and expertise-related constraints and are given as follow.

- The study's spatial extent is confined to the delineated boundaries of Samanabad Town within Lahore, Pakistan, limiting the generalizability of findings to other areas of the city.
- Temporal analysis is delimited to July 2023, thus potentially disregarding seasonal fluctuations and prolonged trends in urban temperature dynamics.
- The computational constraints associated with the InVEST 3.14.2 UCM necessitate the adoption of a number of smaller case study area, potentially simplifying the representation of complex urban landscapes.
- The availability of input data, including land cover classifications and meteorological parameters, may pose constraints on the accuracy of model simulations. LULC classification was solely conducted using satellite imagery, which may introduce uncertainties due to limitations in spatial resolution and classification algorithms.

1.5 SIGNIFICANCE OF STUDY

This study is important because it's doing something new in urban environmental research in Pakistan. To date, no comprehensive validation of the InVEST 3.14.2 UCM has been undertaken in the country. This highlights a notable gap in the literature. Furthermore, there

is a lack of trend toward the adoption of advanced modeling tools and techniques within the urban planning and environmental management sector in Pakistan.

By conducting this study, we are providing empirical evidence of the applicability and efficiency of the InVEST model in representing urban thermal environments within the context of the Pakistan. The results of the research will be essential for advancing the understanding of urban heat mitigation strategies and the role of green infrastructure in mitigating the UHI effect.

The findings of the study have important implications for researchers, practitioners, and policymakers. For researchers, it offers a pioneering exploration into the application of ecosystem services modeling tools in urban environmental management, thus paving the way for future research in the domain of urban planning. Practitioners and policymakers stand to benefit from the insights provided by this study, as it offers evidence-based recommendations for integrating green infrastructure into urban planning and policy frameworks to mitigate heat-related risks and enhance urban resilience.

Moreover, this study has the potential to bridge the gap between academic research and practical implementation in urban planning and policy. By demonstrating the utility of advanced modeling tools like the InVEST model suite, it provides a pathway for urban planners to leverage such technologies to address complex urban environmental challenges effectively. However, it is important to acknowledge that urban planners in Pakistan may lack the necessary skill set to utilize these tools effectively.

2 LITERATURE REVIEW

This section explores climate change and human efforts in this wake, focusing on sustainable development goals and heat mitigation strategies. It delves into the role of advanced modeling techniques in urban planning, the importance of UGS in reducing the UHI effect, and the tools for evaluating and enhancing these green spaces. Significant research and case studies from developed countries are highlighted to showcase effective greening efforts.

The review further identifies research gaps, particularly the lack of comprehensive tools for assessing urban ecosystem services that can be applied globally and cater to the specific needs of countries like Pakistan. It emphasizes the necessity to enhance the knowledge base for urban land-use planning and to integrate natural infrastructure benefits into urban design. Our research aims to fill these gaps by evaluating the cooling potential of UGSs in Lahore at town level.

2.1 CLIMATE CHANGE AND HUMAN EFFORTS

Human-made changes to the landscape, such as increasing impervious surfaces, contribute to the UHI effect (MacLachlan et al., 2021). This phenomenon, a significant challenge in the twenty-first century, leads to higher economic costs, greater energy usage, and negative health effects.

Scientists are finding ways to create hydrogen sustainably, which is commonly made from natural gas. This hydrogen can be used in fuel cells for vehicles and electricity without emitting any harmful gases (Tang & Kemp, 2021). Renewable energy sources like wind, solar, and geothermal power are becoming more popular. In the U.S., they already make up 20 percent of the electricity supply.

There are new technologies being developed to make better batteries for storing renewable energy, improve the electric grid, and capture carbon dioxide emissions from power plants. Some people believe that nuclear power, despite its safety concerns and waste issues, should also be considered as it doesn't produce direct air pollution during operation (Are There Real Ways to Fight Climate Change? Yes., 2024).

Despite the technological solutions, we still need to return to nature and give it back what we have taken from it because we can't live isolated from nature. This discussion further involves different bio-cyclic procedures.

2.2 SUSTAINABLE DEVELOPMENT GOALS

Sustainable Development Goals (SDGs) outlined by the United Nations, particularly those related to sustainable cities and communities (SDG 11), climate action (SDG 13), and life on land (SDG 15) are of great concerns where town planning is concerned.

By validating the effectiveness of the InVEST 3.14.2 UCM in representing urban thermal environments, the study contributes directly to SDG 11, which aims to make cities inclusive, safe, resilient, and sustainable. Specifically, the study addresses Target 11.7 of SDG 11, which focuses on providing universal access to safe, inclusive, and accessible green and public spaces, particularly for women and children, older persons, and persons with disabilities. By assessing the cooling potential of UGS, the study supports the creation of more sustainable and resilient cities, enhancing the well-being of urban residents.

Moreover, the research contributes to SDG 13 by providing empirical evidence of the effectiveness of heat mitigation strategies and green infrastructure in combating the UHI effect and reducing greenhouse gas emissions. This aligns with Target 13.1, which aims to strengthen resilience and adaptive capacity to climate-related hazards and natural disasters in all countries.

Furthermore, the study addresses SDG 15, which focuses on protecting, restoring, and promoting sustainable use of terrestrial ecosystems, combating desertification, and halting biodiversity loss. By examining the impact of urbanization on land surface temperature, vegetation cover, and ecosystem health, the research contributes to Target 15.3, which seeks to combat desertification, restore degraded land and soil, and strive to achieve a land degradation-neutral world by 2030.

2.3 CASE STUDIES OF DEVELOPED WORLD

Here are the few case studies from the developed world as they are moving forward in the race of developing resilience against climate change.

2.3.1 Singapore

Singapore, a city-state situated near the equator, is experiencing rapid warming, heating up twice as fast as the global average while dealing with a high population density. To combat rising temperatures, the city is adopting innovative approaches, blending greenery with advanced building design and technology. Foliage has traditionally been used to cool the urban environment, but now, there's a shift towards strategies like petal-shaped ventilating rooftops and underground cooling systems. The challenge lies in reducing temperatures without significantly increasing carbon emissions, especially in a city with a high reliance on air conditioning (Shaping a Heat Resilient City, 2024).

Despite the benefits of greenery in reducing temperatures, limitations exist, such as reduced wind speed and increased humidity. To address these challenges, Singapore is investing in smart technologies and data modeling, like the digital urban climate twin (Duct), to predict temperature impacts and test different scenarios.

Cooling Singapore 2.0 is centered on the development of a Digital Urban Climate Twin (DUCT) system, employing a network of models to simulate urban environments. This system enables the simulation of various scenarios, allowing for in-depth analysis of their impacts on microclimates (Solving Singapore’s Urban Heat Island Effect, 2024). For instance, the system can model different configurations of vegetation, including variations in size, shape, and density, providing valuable insights into their effects on the surrounding areas' microclimate.

These efforts aim to create more sustainable and resilient urban environments, not just in Singapore but potentially in other cities facing similar challenges. Such models are needed to be developed in the countries that are highly vulnerable to climate change.

2.3.2 Thailand

Recent studies highlights the health and financial risks associated with city flooding due to the mixing of sewage with floodwaters. To address these challenges, the Bangkok-based planning and design firm estudioOCA proposes a vision for Udon Thani as a "green" city, leveraging natural infrastructure like wetlands, trees, and parks to mitigate flooding. Through a year-long project, experts have tested the feasibility of natural infrastructure to absorb

excess water, demonstrating that wetlands and green areas can act as a sponge to reduce flooding by slowing water flow during storms and increasing infiltration (Thailand: Fighting Floods with “sponge Cities” | PreventionWeb, 2024). The passage emphasizes the importance of incorporating wetlands explicitly into urban planning. That’s they theme of Sponge City Concept. Integration of green and blue infrastructure is only going to have better cooling effects on the developed part of the city.

2.3.3 Melbourne

The City of Melbourne’s Grey to Green program idealizes a strategic and incremental approach to repurposing the city to meet the evolving needs of its population over the long term (Green City Case Study: Melbourne, Australia: Grey to Green • AIPH, 2024). In 1985, prioritizing people over cars was considered a radical approach, but it catalyzed a growing awareness of climate change impacts. This approach informed the development of the City’s Urban Forest and Open Space Strategies in 2012, as well as the Nature in the City Strategy and Transport Strategy.

The Greening the City Project is the largest revegetation initiative ever undertaken by the City of Melbourne, aiming to plant approximately 150,000 native trees, shrubs, and grasses to green the city and respond to the COVID-19 pandemic (Greening the City Project - City of Melbourne, 2024). The Melbourne government has hired 10 people to measure the diameter of tree trunks in streets and parks managed by the City of Melbourne. This data is crucial for tracking tree growth rates and determining the necessary canopy growth to reach our canopy cover target. Over a six-month period, approximately 45,000 trees will be surveyed. We can’t imagine having such studies being undertaken in Pakistan.

Studies have been done in Melbourne and they have been rejuvenating their cities by greening and strategic planning efforts. This developed world has been much advanced with development and research and studies have actual on ground implementations. The study by Jamei & Rajagopalan, 2017examined how Melbourne's future urban planning, as outlined in "Plan Melbourne," will impact pedestrian comfort during extreme heat. Using the ENVI-met 3.1 tool, it found that increased building heights and tree canopy coverage slightly improved thermal comfort. Further long-term strategies, like increasing tree canopy coverage to 50%, significantly enhanced pedestrian comfort by reducing temperatures by up to 5.1 °C.

2.4 NOVEL RESEARCH PRACTICES

Models serve multiple purposes in urban planning and policy design (Hamel et al., 2021). Firstly, they inform on-the-ground decisions by providing quantitative assessments with relatively low uncertainty. Secondly, they aid exploration by enhancing understanding of general trends and dynamics in complex systems, helping infer implications of different planning options (Hamilton et al., 2019). Lastly, they facilitate communication and learning by conveying key insights and fostering shared understanding among stakeholders.

Researchers are using sophisticated deep learning and machine learning approaches to tackle complex urban issues. Kajosaari et al., 2024 conducted a study on predicting context-sensitive UGS quality to aid in urban green infrastructure planning, utilizing data from a widespread public participation GIS (PPGIS) survey. Kim et al., 2024 explored the potential of deep-learning algorithms for detecting residential developments in urban areas by using advanced AI techniques to enhance the accuracy and efficiency of urban spatial analysis. Similarly, Jia et al., 2024 conducted research on semantic segmentation of remote sensing images using deep learning, based on the band combination principle, to improve urban planning and land use analysis.

2.5 URBAN GREEN SPACES AND THEIR ROLES

Attributes of the built environment, including urban morphology, vegetative cover, and albedo, are pivotal in the genesis of the UHI phenomenon (Yin et al., 2024). These factors also contribute to intracity thermal heterogeneity. Vegetation plays a crucial role in mitigating the UHI effect by offering shade, altering the thermal characteristics of urban surfaces, and enhancing cooling through evapotranspiration (Urban Cooling | The Natural Capital Project, 2024). Scenario analysis techniques stand out as common approaches for upscaling nature-based Solutions in urban contexts (Cortinovis et al., 2022).

Numerous exemplary projects have showcased the potential of individual, small, and medium-scale UGS in facilitating climate change adaptation. UGS such as green roofs and rain gardens enhance water retention and infiltration, mitigating urban flooding caused by intensified rainfall (Frantzeskaki, 2019). Additionally, they aid in reducing air temperatures through shading and evapotranspiration, thereby alleviating the adverse effects of more frequent and intense heatwaves. These benefits are often accompanied by additional co-

benefits, including recreational opportunities, aesthetic enhancement, improved air quality, social cohesion, and economic prospects.

2.6 ENHANCING AND EVALUATION OF URBAN GREEN SPACES

Expanding the implementation of green solutions may involve integrating them into various levels such as spatial, temporal, jurisdictional, institutional, and management levels, while also broadening networks and knowledge simultaneously (Cortinovis et al., 2022).

2.6.1 Models and Tools for Analyzing Urban Green Spaces

Ecological functions vary in applicability across landscapes; some models, such as those for carbon sequestration and coastal vulnerability reduction, are relevant to both rural and urban areas (Burkhard et al., 2014). Conversely, models like urban cooling and urban flood risk mitigation are tailored specifically for urban environments to address their unique challenges and characteristics.

2.6.2 Tools for the Management of Urban Spaces

Taha, 1997 employed a variant of the URBMET model (Bornstein, 1975) to simulate typical summer conditions in a mid-latitude region with a warm climate, incorporating the effects of surface albedo, evapotranspiration, and anthropogenic heat emissions on the near-surface climatic conditions and recommended the reforestation and augmenting the albedo of roofing and paving material.

2.6.3 Tools for Analyzing Cooling Capacity

Zhang et al., 2024 compared 50 urban parks in China's temperate monsoon climate, finding 90% significantly lowered LST. Park characteristics, especially size, notably influenced cooling effects, suggesting prioritizing parks with high cooling efficiency and intensity for optimal urban cooling benefits.

- **ENVI MET, UMEP**

ENVI-met is able to replicate the lack of significant cooling effects during the daytime and only marginal cooling at night as given in a study by Scharfstädt et al., 2024. To tackle these

challenges, they examined various mitigation scenarios, incorporating heat mitigation strategies.

- **Utilization of INVEST UCM**

Ronchi et al., 2020 investigated how ecosystem services assessment could inform the definition of urban design parameters that influence the CC of cities. He used InVEST UCM for urban design analysis of city of Milan and did the performance-based morphological analysis.

The research by Hamel et al., 2023 developed and calibrated an algorithm for the UCM in the InVEST software, estimating temperature reduction by vegetation using four predictors. It evaluated the model in Paris and Minneapolis-St Paul, showing high nighttime air temperature accuracy but lower daytime accuracy, and successfully simulated a green infrastructure scenario in Paris for urban planning.

This model has also been used for assessing climate vulnerability and heat mitigation. For instance, the study by (Keyes et al., 2022) used the InVEST Model to assess heat mitigation in Milwaukee. It found central and northwest Milwaukee, primarily Black and Latine communities, have low heat mitigation and high heat vulnerability, with increased tree canopy shown as an effective mitigation strategy.

A study by Carrasco-Valencia et al., 2024 utilized the Water Yield model of InVEST to evaluate water yield (WY) changes in Arequipa, Peru, due to urbanization near the Chili River. Results showed an increase in urban area contribution to WY, from 30.43% in 1984 to 49.62% in 2022, mitigating total WY loss due to higher runoff rates and surface flow caused by urban expansion.

- **Integration of Other Tools with InVEST**

The model has been jointly used with others. In the research by Zhou et al., 2023, they modeled urban cooling service flow (UCSF) within Beijing's 6th Ring Road using the InVEST tool and a Gaussian function, analyzing landscape patterns' contributions to UCSF with Fragstats and GeoDetector. Another study by Hamel et al., 2021 used a blend of InVEST and custom models and showed a 0.4% reduction in natural and semi-natural areas in Ile-de-France over the past 35 years.

- **Features of InVEST**

The InVEST model stands out for its versatility and accessibility, designed to be applicable in cities worldwide regardless of data availability or resource constraints. This adaptability is crucial for cities with limited data and resources to run complex models, making it an invaluable tool for urban planning and decision-making (Bosch et al., 2021). Additionally, the growing accessibility of high-resolution environmental data through global earth observations enhances the model's capabilities by improving spatial data inputs and model parameters, further increasing its effectiveness in diverse urban contexts.

Research by SSRN-Id4730369, 2024 focused on Poitiers' urban landscape, aiming to locate heat areas using two methods (cooling index modeling and satellite data comparison). Results revealed a significant correlation between methods, indicating the effectiveness of heat mapping even without satellite data. Thus, InVEST model can even work without the need for high resolution satellite imagery.

2.7 GAP IN LITERATURE

Alternative tools commonly used for urban ecosystem service assessment include i-Tree, Urban Multi-scale Environmental Predictor (UMEP), ARIES (Artificial Intelligence for Ecosystem Services), Costing Nature, UrbanBEATS (A Planning-Support System for Blue Green Cities), and SolVES (Social Values for Ecosystem Services). These tools have significantly advanced the measurement of natural infrastructure benefits in cities worldwide (Hamel et al., 2021). However, none of them can simultaneously assess a wide range of urban ecosystem services, work in cities globally, and inform various urban decision contexts (e.g., flood zone planning, climate adaptation, biodiversity conservation, and public health). Further they require multitudes of data that might not be available for Pakistan and can only be operated for US and Europe. Some aren’t open to public and aren’t freely available.

UrbanBEATS in union with SSANTO Planning-Suppose System can be a really smart smart tool for the management of blue and green spaces of the city. It’s still at the growing stage and limited research has been done (UrbanBEATS – A Planning-Support System for Blue Green Cities, 2024).

Nice et al., 2024 conducted the study that assesses the cooling potential of additional Blue-Green Infrastructure (BGI) enabled by Integrated Water Management (IWM) across major

Australian cities using the TARGET model, designed to evaluate heat mitigation benefits and predict air and surface temperature patterns at the neighborhood to city scale.

Some softwares and tools require long procedures. While UMEP does require some level of technical expertise and data availability, it's designed to be user-friendly and adaptable to various contexts. Its effectiveness in Pakistan highly depends on data availability, local knowledge, and the expertise of the user (UMEP Manual — UMEP Manual Documentation, 2024). It has been used in integration with InVEST model in the past researches. Thesis has been done on the integration of cooling models and UMEP applications (Belinda Puspita, 2024).

i-Tree focuses on urban trees and cannot assess benefits from green roofs or coastal habitats. Also, it can't be used for countries like Pakistan due to limited availability of data (I-Tree Tools - Calculate the Benefits of Trees!, 2024). Many tools arise from specific fields and target a narrow set of services, such as stormwater management. Comprehensive assessment of services and natural infrastructure is crucial for advancing urban system science and promoting dialogue between researchers and practitioners from diverse fields.

2.8 NEED FOR FURTHER RESEARCH

Presently, there is a deficiency in information regarding the ecosystem services provided by urban regions, highlighting the necessity to enhance the knowledge base for land-use planning (Niemelä et al., 2010). Despite recent progress, urban decision-makers still face challenges in integrating natural infrastructure benefits into urban design and planning (Hamel et al., 2021). Additionally, the potential spatial association effect of UGS demands attention (Wang et al., 2024). Given the rising thermal pressures on urban areas due to climate change, a precise evaluation of UGSs' ability to alleviate the heat island effect is vital for informed planning decisions (Battisti et al., 2024). However, such assessments often necessitate data that may not be readily available to planners.

3 METHODOLOGY

This section of the research outlines the procedures adopted to conduct the study. It includes details on the study area, materials, and methods used. The section further covers the inputs required for LULC classification, such as building footprints, satellite imagery, NDVI, NDWI, and NDBaI along with their resources. Additionally, it explains how the accuracy assessment of image classification was carried out using Confusion Matrix and Kappa Coefficient.

It further gives insight into the InVEST UCM, detailing the inputs needed for the model, including land use classification, reference evapotranspiration, green area maximum cooling distance, building footprints, UHI effect, blending distance, reference air temperature and biophysical table. It also discusses what will be the outputs of the model, including CC, Evapotranspiration Index (ETI), and the HMI, as well as the verification methods involved for the validation of these outputs.

3.1 STUDY AREA

Lahore is the second largest city of Pakistan situated in the north-eastern part of the country, between 31°15′—31°45′ N and 74°01′—74°39′ E. It is bounded by the Sheikhupura District to the north and west, Wagah to the east, and Kasur District to the south. The Ravi River flows on the northern side of the city. City has the area of 1772 km^2 with a population of over 13 million, ranking it among the top megapolis of the world (Welcome to Lahore | Lahore, 2024).

It has a semi-arid climate with warm weather throughout the year, characterized by hot summers and mild winters. It has been administratively divided into nine towns, which are further subdivided into 150 Union Councils (UCs). Samanabad Town has been chosen as the case study area spread across 38.34 km^2 with approximate 1,073,629 people living in the locality in 2014 as per the records of Lahore Population Density Map PDF | Geomatics, 2024.

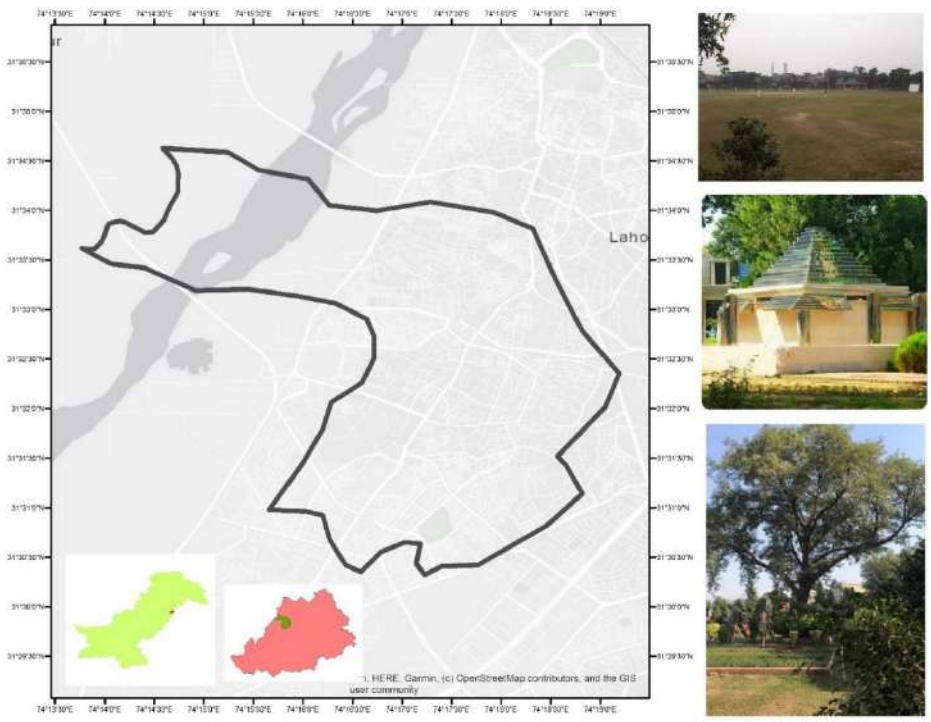

Figure 3.1: Case Study Area: Samanabad Town, Lahore (Author, 2024)

3.2 MATERIALS AND METHOD

The section elaborates on the processes involved in acquiring and verifying data, as well as providing background information on the methodologies employed in the models utilized for the research.

3.2.1 Inputs Required For LULC

To ensure accurate classification of LULC with a focus on vegetation distinctions, a unique approach was adopted due to limited availability of suitable data from online sources. Traditional satellite images from sources like Landsat and Sentinel were not utilized due to their relatively low resolution (30 meters and 10 meters respectively) and inability to provide clear differentiation between vegetation types. Instead, a combination of data sources was integrated and overlaid to generate comprehensive LULC data. This included high-resolution imagery obtained through alternative means, such as detailed satellite imagery from SAS Planet and Google Earth Engine (GEE), which offered clearer delineation of vegetation boundaries. Additionally, ancillary data layers, such as spectral indices like NDVI and NDWI, were incorporated to enhance the classification process. Subsequently, accuracy

assessment procedures were employed to evaluate the reliability and quality of the generated LULC dataset, ensuring its suitability for further analysis and modeling. The data acquisition process and sources are explained in detail below.

- **Building Footprint**

To extract building footprints with multiple confidence levels from high-resolution imagery for Lahore, Pakistan, we employed a simple yet effective approach. This method utilizes GEE, a cloud-based platform for analyzing geospatial data, to filter and merge building polygons based on their confidence levels.

First, it defines a feature collection ('GOOGLE/Research/open-buildings/v3/polygons') and filters it based on a specified region of interest (ROI). The string 'GOOGLE/Research/open-buildings/v3/polygons' is a reference to a dataset available within GEE. Specifically, it refers to a dataset containing polygon features representing buildings. This dataset is the part of Google's research initiative focused on mapping and analyzing building footprints using satellite imagery and machine learning algorithms (Sirko et al., 2021).

The buildings are then divided into three categories based on their confidence levels: low (0.65 - 0.7), medium (0.7 - 0.75), and high (>= 0.75). Next, a function is defined to remove problematic properties from the features, particularly the geometry property. Each filtered collection is then mapped with the function to remove the geometry property. Finally, the filtered collections are merged into one single collection, and layers representing each confidence level are added to a map interface. Additionally, the merged collection is exported as a shapefile. Later the layer was rasterized in order to be overlayed with other layers.

- **Satellite Imagery**

To acquire high-resolution satellite imagery from Google Maps, we utilized the SAS. Planet application, which serves as a gateway to accessing various map sources. Within SAS. Planet, we navigated to the specific area of interest and selected Google Maps as the provider. We chose a zoom level of 19 to ensure the desired level of detail suitable for our analysis. We tried increasing the zoom level but the process was time taking.

The selected tiles were then stitched together, resulting a single image that was later saved in GeoTIFF file format, which preserves georeferencing information and ensures compatibility with various GIS software and analysis tools.

- **NDVI**

The Normalized Difference Vegetation Index (NDVI) is the most commonly used remote sensing index that measures and monitors vegetation health, cover, and growth. It is particularly valuable in agricultural monitoring, environmental studies, and land management (J. Chen et al., 2004). Here we used it to identify dense and moderate vegetation. The vegetated layer was extracted later to combine with others. Landsat 8 data was used from the date of 26th July, 2023. NDVI was calculated using the following formula.

$$NDVI = \frac{(NIR - RED)}{(NIR + RED)} \quad 3.1$$

- **NDWI**

The Normalized Difference Water Index (NDWI) is used to identify and monitor water bodies such as lakes, rivers, and wetlands. It enhances the presence of water features while suppressing the influence of vegetation, soil, and other land covers. The NDWI is particularly useful in hydrological studies, flood monitoring, and water resource management (Gao, 1996). Water layer was extracted from this index. Same Landsat imagery was taken as mentioned above. NDWI has the following formula.

$$NDWI = \frac{(Green - NIR)}{(Green + NIR)} \quad 3.2$$

- **NDBaI**

The Normalized Difference Barren Index (NDBaI) is used to identify barren land areas, such as bare soil, sand, and rocks. It is useful in environmental monitoring, LULC mapping, and assessing desertification processes. The index is calculated using specific bands from satellite imagery, typically from sensors like Landsat (Hung, 2020). Its value ranges from -1 to 1, with higher values indicating barren land and lower values indicating non-barren areas (e.g., vegetation, water). Same Landsat 8 data was taken. Here is the formula for its calculation.

$$NDBaI = \frac{(\text{SWIR1} + \text{RED}) + (\text{NIR} + \text{BLUE})}{(\text{SWIR1} + \text{RED}) - (\text{NIR} + \text{BLUE})} \quad 3.3$$

Where:

- SWIR1 is the shortwave infrared band (usually around 1.55–1.75 µm).
- RED is the red band (around 0.64–0.67 µm).
- NIR is the near-infrared band (around 0.85–0.88 µm).
- BLUE is the blue band (around 0.45–0.51 µm).

3.2.2 Accuracy Assessment of Image Classification

The methods of accuracy assessment for Land Use/Land Cover (LULC) classification include visual interpretation, ground truth data collection, and comparison with reference data. Field surveys is a time taking process require considerable time. The confusion matrix is the most utilized and convenient method, quantifying the agreement between the classified and reference LULC maps by tabulating the number of correctly and incorrectly classified pixels for each land cover class.

- **Confusion Matrix**

In ArcGIS, a confusion matrix for Land Use/Land Cover (LULC) classification is typically generated by comparing the classified LULC map produced by a classification algorithm or model with a reference (ground truth) LULC map. Sample points representing various land cover types are generated across the study area using tools like the "Create Random Points" tool. These sample points are then visually inspected to assign the corresponding land cover class based on the reference data.

The classified LULC map is then compared to the Google Earth Pro Satellite Imagery, and each pixel's classification is recorded in the confusion matrix. The confusion matrix tabulates the number of correctly and incorrectly classified pixels for each land cover class. Finally, accuracy assessment metrics such as overall accuracy, producer's accuracy, and user's accuracy are calculated from the confusion matrix to evaluate the performance of the classification algorithm.

We utilized Python and imports necessary libraries such as matplotlib for plotting and numpy for numerical operations. It employs scikit-learn, a machine learning library, specifically for metrics like confusion matrix computation. This script takes actual and predicted values as

input, computes the confusion matrix, and then visualizes it using matplotlib's ‘metrics.confusion_matrix’ function. Finally, the plot was saved as an image.

- **Kappa Coefficient**

The Kappa coefficient, also known as Cohen's Kappa, is a statistical measure used to assess the level of agreement between two sets of categorical data (Vieira et al., 2010). In the context of LULC classification, the Kappa coefficient is a statistical metric used to evaluate the accuracy and agreement of a classification algorithm or model in correctly assigning land cover categories to pixels on a map. It quantifies the level of agreement between the classified map and a reference (ground truth) map, accounting for agreement occurring by chance. A higher Kappa coefficient indicates a higher level of agreement and accuracy in the classification process. This will be telling us if our generated land use classification map is accurate enough or not.

3.2.3 INVEST Urban Cooling Model

The assessment was conducted using the UCM of InVEST software (Integrated Valuation of Ecosystem Services and Tradeoffs, version 3.14.2), an open-source modeling suite designed to aid decision-makers in integrating CC and HMI into various policy and planning contexts, including spatial planning, strategic environmental assessment, and environmental impact assessment (Urban Cooling | The Natural Capital Project, 2024).

InVEST, developed collaboratively by Stanford University, the University of Minnesota, the Nature Conservancy, and the World Wildlife Fund, is freely available for download from the Natural Capital Project website. This model calculates HMI by integrating evapotranspiration from vegetation, the cooling influence of large urban parks, and albedo from land cover maps to quantify the average cooling effect on air temperature. It combines geographical, economic, and ecological data to support regional and urban planning, aiming to restore and maintain the capacity of ecosystems to provide essential services.

3.2.4 Inputs Required for InVEST Model

The model utilizes spatially explicit raster and vector maps as inputs to represent the ecosystem under study. It produces outputs in the form of maps, biophysical quantities, or economic terms (Kadaverugu et al., 2021). The UCM uses various factors such as

evapotranspiration from plants, the cooling impact of big city parks, and the reflection of sunlight from different surfaces (albedo) to measure the overall cooling impact on the surrounding air temperature (Battisti et al., 2024). It also uses the building footprint data and the method of data acquisition has already been explained in the previous section.

No accurate and precise data has been available for the region including the data on CC. Firstly, the model computes the CC index, which is based on the physical mechanisms that contribute to cooling urban temperatures, for each pixel based on local shade, ET_0, and albedo and then it computes the CC of green areas and water bodies (if added). This information is important for guiding municipalities and stakeholders in improving strategies and implementing nature-based strategies to mitigate the UHI effect.

The HMI along with the CC required the following inputs for its calculation. The model has been used by Battisti et al., 2024; Bosch et al., 2021; Hamel et al., 2021, 2023; Kadaverugu et al., n.d.; Kajosaari et al., 2024; Keyes et al., 2022; Ronchi et al., 2020 and Zawadzka et al., 2021a, 2021b for various scenarios and multiple case studies. Also, we generated four different scenarios. Details of the inputs given to the model are given below.

- **Land Use Classification**

The area selected includes the boundary of Samanabad Town, designated as Area of Interest (AOI), was provided as our input shapefile in raster format. The LULC map, elaborated in the previous section, was provided to ensure accurate representation of land cover classifications, which are essential for modeling the CC and understanding the impact of different land uses on urban heat mitigation. Here, we generated four different scenarios. Initially, our raster LULC map had a spatial resolution of less than one meter. Model was taking 4 days to run a single simulation. Hence, the pixel size was reduced and firstly, we took the resolution of 10 meters and then it was also resampled to 20 meters.

- **Reference Evapotranspiration (ET_0)**

It quantifies the amount of water that evaporates from the land surface into the atmosphere over a specified period. It is typically measured as the depth of water in millimeters (mm) over a given time frame (Hu et al., 2023).

The MOD16A2 Version 6.1 Evapotranspiration/Latent Heat Flux product, sourced from MODIS, is an 8-day composite product at a 500-meter pixel resolution. It utilizes the

Penman-Monteith equation and includes daily meteorological reanalysis data and MODIS remotely sensed data. Open-source data on Evapotranspiration/Latent Heat Flux is provided by NASA LP DAAC at the USGS EROS Center. GEE was used for data collection and filtering was done using JavaScript. Data contained evapotranspiration values (in millimeters) over the last 24 years from January 1, 2000 to May 1, 2024. Methodology was adopted from Sidhu et al., 2018.

In our study, we employed a methodology that involved harnessing the power of various Earth Observation (EO) datasets to estimate evapotranspiration (ET) across a designated region, known as ET_region. This process encompassed several pivotal steps aimed at processing and analyzing data sourced from multiple EO platforms. Initially, we imported a shapefile delineating the boundaries of the study area (ET_region) into the GEE platform and subsequently centered the map display on this specific region for visualization purposes.

Our dataset selection process was focused on EO datasets renowned for their reliability. These datasets included GLDAS (Global Land Data Assimilation System), MODIS (Moderate Resolution Imaging Spectroradiometer), TerraClimate, SMAP (Soil Moisture Active Passive), and PML (Penman-Monteith-Leuning). Each dataset was chosen based on its unique temporal and spatial resolutions, as well as its specific parameterization methods for ET estimation as described in the past studies.

The data processing workflow involved several key stages for each selected dataset and all of this has been done through GEE and python script. Firstly, we determined the temporal range available for analysis by calculating the difference in months between the earliest and latest dates within each dataset. Next, we computed monthly mean ET values to standardize the data across different temporal resolutions. This involved iteratively filtering the dataset for each month and calculating the mean ET value for that specific month. Additionally, we performed unit conversion to ensure consistency in the ET values, converting them to a common unit of measurement (mm/day).

Visual representation of the processed data was important so we generated time series charts to depict the monthly mean ET values derived from each dataset. These charts facilitated the visualization of temporal trends in ET over the study period and were useful in providing insights into the ET dynamics within the region. The charts were generated using GEE's

charting capabilities, with each dataset's time series plotted to showcase mean ET values for each month, spatial averaging over the ET_region, and appropriate scaling factors based on the dataset's resolution.

Specific implementations were kept unique. For instance, GLDAS data were aggregated to monthly averages and converted from kg/m²/s to mm/day. Similarly, MODIS data, available at both 1 km and 500 m resolutions, were processed into 8-day composite periods and converted to mm/day. TerraClimate monthly data underwent appropriate scaling, while SMAP high temporal resolution data were aggregated to monthly means. The PML dataset, featuring multiple ET components, underwent similar processing, with all components aggregated and visualized accordingly.

- **Green Area Maximum Cooling Distance (d_{cool})**

This distance is expressed in meters, representing the maximum cooling effect distance of large green areas or it was defined as a distance till the UGS has a cooling effect by Kadaverugu et al., 2021. These effects decrease with distance from green spaces.

This was estimated based on methodology proposed by Jaganmohan et al., 2016. For Samanabad Town, green spaces were relatively small and dispersed with limited management. So, a cooling effect distance of 100 m and then 200 m was selected for the AOI.

- **Magnitude of the UHI Effect (UHI_{max})**

We needed the maximum value for the model, so the UHI was computed in order to see the maximum value on the specific day. UHI represents the temperature difference between the rural reference temperature and the maximum temperature observed in the city. Data was derived from the Landsat imagery processing on the date of 26th July, 2023.

To process Landsat 8 satellite imagery for our study area, we developed a series of custom functions in GEE. The first function, "applyScaleFactors," was designed to apply scale factors to the image bands, specifically addressing the optical and thermal bands. This step involved converting the raw digital numbers of the bands into physical units, ensuring consistency and accuracy in subsequent analysis.

Next, we implemented a cloud masking function, "maskL8sr," to remove pixels affected by clouds and cloud shadows from the imagery. This process involved identifying and masking out areas with cloud cover using information from the pixel quality assessment (QA) band.

Following the preprocessing steps, we filtered the Landsat 8 image collection based on the specified date range and AOI. This filtering ensured that only relevant images within the desired temporal and spatial extent were included in our analysis. We then applied the previously defined scale factors and cloud masking function to each image in the collection. the data from the thermal band (i.e., band 10) of Landsat imagery were first converted to top-of-atmosphere spectral radiance (L_λ) masked to AOI. Brightness values has been calculated then with the following formula.

$$\mathrm{BT} = \frac{K_2}{\ln((K_1/L_\lambda)+1)} - 273.15 \tag{3.4}$$

Here, K_1 and K_2 are band-specific thermal conversion constants embedded in the Landsat image metadata and can be found in the txt file downloaded from USGS or the values can be simply extracted from GEE. To create visualizations, we generated a true-color composite and calculated the NDVI from the preprocessed imagery. Additionally, we derived vegetation-related indices such as the Fraction of Vegetation (FV) and the Emissivity (EM) from the NDVI values. For these, we have the formulas as follow.

$$\mathrm{FV} = \left(\frac{(\mathrm{NDVI} - NDVI_{min})}{(NDVI_{max} - NDVI_{min})}\right)^2 \tag{3.5}$$

$$EM = FV \times 0.004 + 0.986 \tag{3.6}$$

For thermal analysis, we calculated the LST using the thermal band of the Landsat 8 imagery. This involved applying a radiative transfer equation to convert the brightness temperature to LST, considering factors such as emissivity and atmospheric conditions. Formulas for LST and UHI are given as follow.

$$\mathrm{LST} = \frac{T_b}{1 + (0.00115 * \left(\frac{T_b}{EM}\right) * \log EM} - 273.15 \tag{3.7}$$

ere T_b is the brightness temperature (thermal band) of the Landsat imagery.

$$UHI = \frac{LST - Mean\ LST\ in\ AOI}{STD\ LST\ in\ AOI} \quad 3.8$$

Highest value of UHI was recorded for the input.

- **Air Temperature Maximum Blending Distance**

It is a search radius (in meters) used in the moving average to account for air mixing. This parameter has been added to the model to solve the wind dynamics in small areas (Hu et al., 2023). The model utilizes a temperature dispersion parameterization to address the meteorological mixing of air temperature (Tair) across the study area. This is achieved by incorporating a blending distance (dair), with a default value set at 2000 meters (Kadaverugu et al., 2021).

- **Reference Air Temperature**

We used the lowest average temperature recorded on July 26th of 2023 around our case study area.

- **Biophysical Table**

This table have to be provided as an input to the model. This is the mapping of each LULC code (code must be a unique integer) to biophysical data for that specific LULC class. All values in the LULC raster must have corresponding entries in this table. The table in cooperates the following elements.

Albedo: It is the proportion of solar radiation that is directly reflected by the specific LULC class. It's considered as an important factor for heat reduction based on the research by Kunapo et al., 2018 and Zardo et al., 2017. The albedo of a surface denotes its hemispherical and spectrally integrated reflectivity, encompassing both homogeneous and heterogeneous configurations (Taha, 1997). Urban albedo typically falls within the range of 0.10 to 0.20; however, exceptions exist where these values are exceeded within specific urban locales.

Albedo for urban built infrastructure can be found in local microclimate literature as provided by Bartesaghi Koc et al., 2018. These values were taken from the studies by Zawadzka et al., 2021 and Kadaverugu et al., 2021 and spatial map was generated by the InVEST UCM. A

study implies that an increase of 0.1 in albedo could potentially lead to a decrease of around 2°C in LST and this is consistent with the results of (Yin et al., 2024).

Shade: Shade represents the proportion of tree cover, with values between 0 and 1 (Ronchi et al., 2020). It represents the proportion of tree cover of each LULC class (Kunapo et al., 2018).

Crop Coefficient (Kc): Crop or evapotranspiration coefficient has the value between 0 and 1, calculated based on the studies conducted by Zawadzka et al., 2021 and Kadaverugu et al., 2021.

Green Area: whether the land use class should be considered a green area or not. We took all green spaces as well as water as 1 and the rest of the land uses were assigned the value zero. Green areas larger than 2 hectares have an additional cooling effect.

- **Additional Inputs**

While the model allows for the inclusion of data on building energy consumption, the data available for this study was not sufficiently accurate. Therefore, the model was run without these additional inputs.

3.2.5 InVEST Urban Cooling Model

Outputs of the model are listed as follow.

- **Tree Shading**

Tree shading is calculated by overlaying a binary tree canopy mask with the rasterized LULC map. For each LULC class k, the shade coefficient is determined as the average proportion of tree cover across all LULC pixels of class k, as follows:

$$S_k = \frac{1}{|\Omega_k|} \sum_{j \in \Omega_k} x_j \qquad 3.9$$

Here, Ω_k represents the set of pixels in the tree canopy mask that correspond to class k in the LULC raster (Kunapo et al., 2018). The value x_j indicates whether pixel j in the tree canopy mask corresponds to a tree (value of one) or not (value of zero).

- **Evapotranspiration Index (ETI)**

The ETI is computed as a normalized value of the potential evapotranspiration as follow.

$$\mathrm{ETI} = \frac{K_c \cdot \mathrm{ET}_{ref}}{\mathrm{ET}_{max}} \quad 3.10$$

Where:

- K_c is the evapotranspiration coefficient,
- ET_{ref} is the reference evapotranspiration raster for the period and AOI,
- ET_{max} is the maximum evapotranspiration value observed in the AOI.

- **Albedo Coefficient**

The albedo coefficients are based on the local climate zone classification and has been generated by the model as output.

- **Cooling Capacity Index**

CC is regarded as one of the most fundamental urban ecosystem services (ES), offering numerous health benefits (Ronchi et al., 2020). It can model and identify the most suitable land use and define successful urban design parameters aimed at enhancing human well-being. is It is explained as the ability of urban green areas to mitigate and reduce the impact of heat waves in highly urbanized contexts (Ahmadi Venhari et al., 2017).

It was calculated by the following formula.

$$CC = 0.6 * S + 0.2 * ETI + 0.2 * A \quad 3.11$$

- **Cooling Capacity Index of Parks**

To account for the cooling effect of large green spaces, the computed CC index of pixels within large green areas (> 2 ha) is adjusted as follows.

$$\mathrm{CC}_i^{\mathrm{green}} = \sum_{j \in \Omega_i} g_i \cdot \mathrm{CC}_j \cdot e^{-\frac{d(i,j)}{d_{\mathrm{cool}}}} \quad 3.12$$

where gi is one if pixel i is a green area and zero otherwise (as defined in the biophysical table), d(i,j) is the distance between pixels i and j, d_{cool} is a parameter defining the distance over which a green space has a cooling effect, and Ω_i is the set of pixels within d_{cool} of pixel i.

- **Heat Mitigation Index (HMI)**

To incorporate the cooling effects of large green spaces (>2 ha) on their surroundings (Zardo et al., 2017), the UCM calculates the HMI. If a pixel is not influenced by large green spaces, the HMI is equal to the CC. However, if the pixel is affected by large green spaces, the HM index is determined as a distance-weighted average of the CC values from both the large green spaces and the pixel itself.

This index is used to estimate a temperature reduction by vegetation.

$$HMI_i = \{CC_i\ , if\ CC_i > CC_{park_i} or\ GA_i < 2ha\ CC_{park_i}\ otherwise\} \quad 3.13$$

Where GA_i is the amount/number of green areas within a search distance d_{cool} around each pixel

$$GA_i = cell_{area} \cdot \sum_{\substack{j \in dradius \\ fromi}} g_j \quad 3.14$$

3.2.6 Verification and Insights from Outputs

In this study, we compared the heat mitigation maps derived from the InVEST 3.14.2 UCM with LST data available for July 26, 2023, for the AOI. Maps were geenrated and resampled at two spatial resolutions: denoted as 10 and 20 m for LST. The coarser resolution LST image was acquired from Landsat 8 thermal infra-red bands. Its mixed spatial resolution arises because Landsat 8 thermal infra-red data are captured at 100 m resolution and subsequently resampled to 20 m resolution. Conversely, the finer resolution image was generated from the Landsat 8 LST map through a downscaling procedure.

The comparison between the CC and LST data was conducted using ordinary least squares (OLS) linear regression within the built-up area boundary manually digitized from aerial imagery. Resampling of the 10 m resolution maps to 20 m resolution enabled direct comparisons with 20 m resolution LST datasets using linear regression, as both maps

captured thermal responses of all land cover types within the coarse-resolution pixels without requiring multiple regression accounting for each land cover type located within the pixels. Ultimately, four HMI maps were generated for AOI, accommodating two different cooling distances from large vegetated patches (100 and 200 m).

4 FINDINGS

This section presents the results of our research, focusing on the outcomes and inputs of the model we used. This includes all the maps we generated, such as the LULC classification, as well as the inputs. It is discussed how the heat mitigation maps and CC data is compare to LST. This comparison will help us understand how different urban features affect local temperature.

4.1 INPUTS FOR LULC AND FINAL MAP

The analysis of spectral indices for LULC classification reveals significant variability across the study area. The NDVI ranges from -0.164 to 0.77, indicating varying levels of vegetation density. Higher NDVI values (greater than 0.5) is signifying denser vegetation, while negative values suggest non-vegetated surfaces like water bodies and urban areas.

Similarly, the NDWI ranges from 0.198 to -0.68. Positive NDWI values are associated with water features, while negative values indicate non-water surfaces. The NDBaI varies from 0.0094 to 0.41, indicating the presence of barren land as observed around the river.

The LULC map was generated primarily based on vegetation-based classes. No such map was previously available for Lahore despite being the second largest city of Pakistan. So, we divided the area into seven distinct classes.

- Trees: This category includes areas covered by forests, urban forest, and other vegetated land predominantly characterized by tree cover. The observation of graveyards suggested that they are densely covered with trees.
- Buildings: It encompasses all man-made structures such as residential, commercial, industrial buildings and such other urban developments.
- Grass: This class comprises open areas covered with grass, including lawns, parks, and such other public open spaces.
- Paved areas: It includes surfaces covered with concrete, asphalt, or other solid materials, such as roads, parking lots, and sidewalks.

- Water bodies: This category represents natural or artificial water features like rivers, lakes, ponds, reservoirs, and canals. Ravi River and few ponds in public parks were identified as exiting water bodies.
- Agricultural land: It covers areas used for farming, cultivation, and agricultural activities.
- Vacant land: This class includes undeveloped or unused land devoid of significant vegetation or structures.

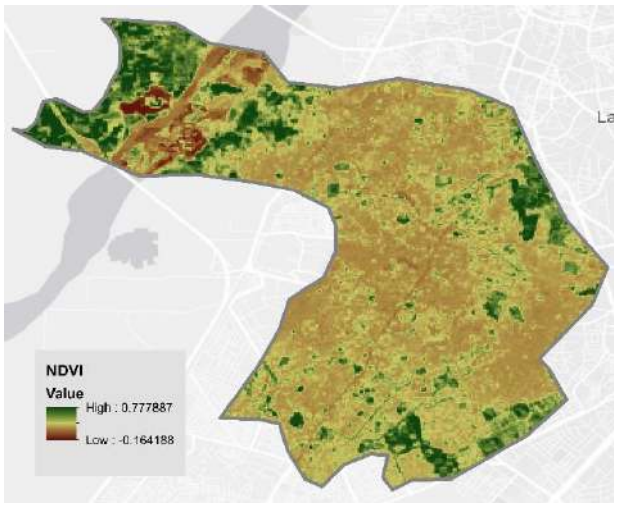

NDVI

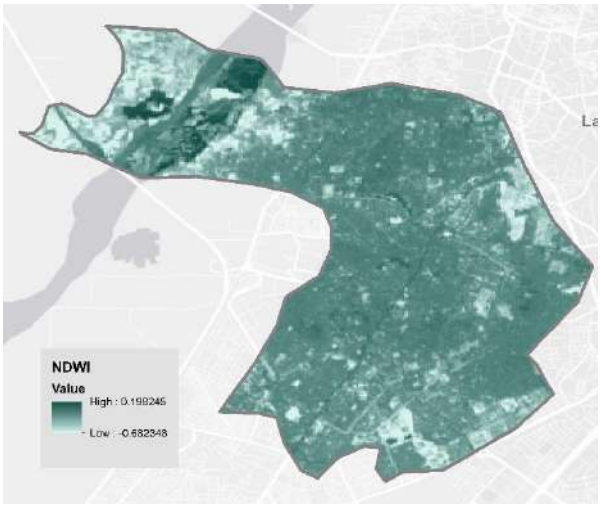

NDWI

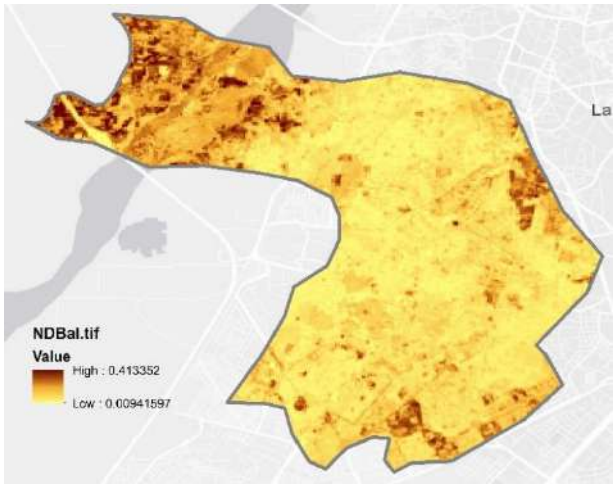

NDBaI

Imagery from SAS Planet

Figure 4.1: Input Required for LULC Map (Author, 2024)

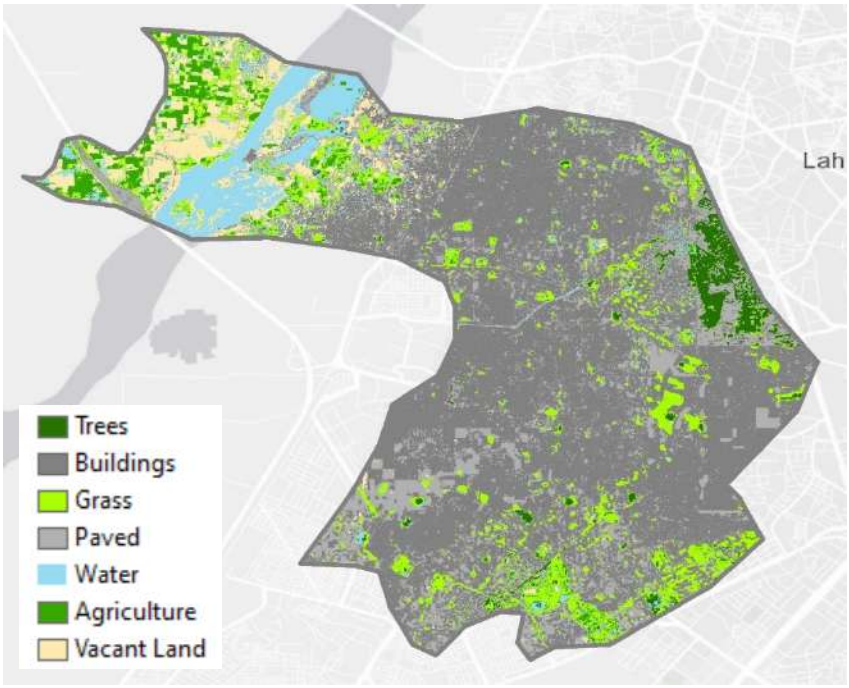

Figure 4.2: Land Use Land Cover Map (Author, 2024)

4.2 ACCURACY ASSESSMENT FOR LULC

For accuracy assessment of LULC, specific points were marked and are highlighted in the provided image. These points serve as reference locations for evaluating the precision of land cover classification within the study area. The marked points enable a comparative analysis between the classified land cover types and ground truth observations.

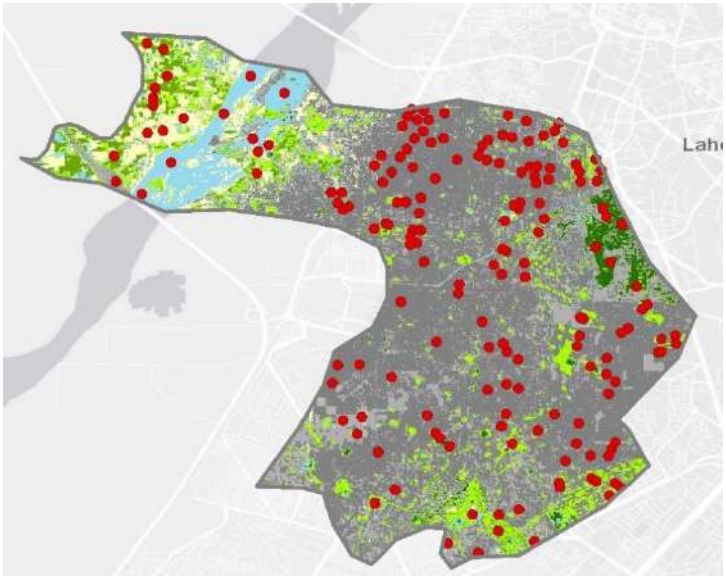

Figure 4.3: Accuracy Assessment Points (Author, 2024)

4.3 CONFUSION MATRIX

The table was generated in ArcGIS and Kappa coefficient was estimated. The labels C_1 to C_7 correspond to the following land cover classes: Trees, Buildings, Grass, Paved areas, Water bodies, Agricultural land, and Vacant land, respectively. For example, in the "Trees" row, it shows that 17 instances were correctly classified as trees, while 2 were mistakenly classified as something else. Trees were the headrest to identify. ArcGIS Pro “Deep Learning Libraries” has been tried for the identification of tree canopy but the algorithm wasn’t that efficient. It was detecting a few buildings as trees too. Overall, the accuracy of the model, which tells us how often it was correct across all classes, is 84%, which is pretty good. The Kappa coefficient, another measure of accuracy, is 79%, indicating strong agreement between the model's predictions and the actual data.

Table 4.1: Accuracy Assessment Results

ClassValue	C_1	C_2	C_3	C_4	C_5	C_6	C_7	Total	U_Accuracy	Kappa
C_1	17	0	2	0	0	0	0	19	0.89	0
C_2	0	72	0	4	0	0	0	76	0.95	0
C_3	11	1	23	1	0	0	0	36	0.64	0
C_4	1	5	0	16	0	0	0	22	0.73	0
C_5	0	0	0	0	6	0	0	6	1.00	0
C_6	1	0	1	0	0	8	0	10	0.80	0
C_7	0	0	0	0	0	0	5	5	1.00	0
Total	30	78	26	21	6	8	5	174	0.00	0
P_Accuracy	0.57	0.92	0.88	0.76	1.00	1.00	1.00	0.00	0.84	0
Kappa	0	0	0	0	0	0	0	0	0	0.79

Source: (Author, 2024)

We generate a confusion matrix to assess the accuracy of a classification or prediction model by comparing predicted values to actual values across different classes. This matrix provides a summary of correct and incorrect classifications, aiding in the evaluation of the model's performance and identifying areas for improvement in classification accuracy.

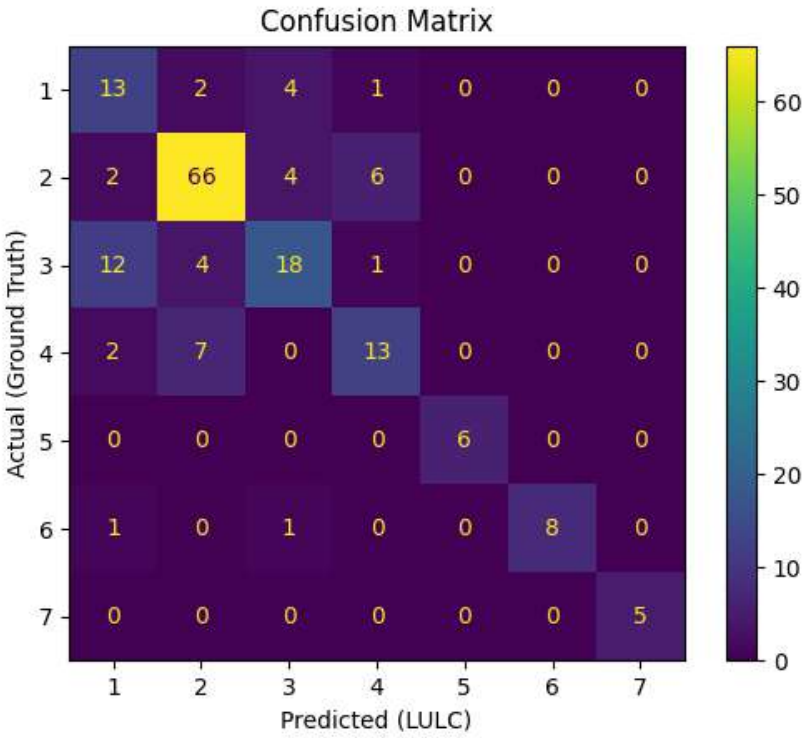

Figure 4.4: Confusion Matrix (Author, 2024)

4.4 BIOPHYSICAL TABLE

This table outlines the biophysical attributes associated with different land cover types utilized in the LULC classification model. Each row corresponds to a distinct land cover class, such as trees, buildings, grass, paved areas, water bodies, agricultural land, and vacant land. The columns represent specific characteristics of these land cover types, including shade, crop coefficient (Kc), albedo, the presence of green areas, and building intensity.

For example, in the "Trees" category, the shading coefficient is 1, indicating full shade, the Kc value is also 1, suggesting high rates of evapotranspiration typical of healthy vegetation, the albedo is 0.15, indicating moderate reflectivity, green areas are present (value of 1), and there is no building intensity (value of 0).

Similarly, each land cover class is distinguished by these parameters, aiding in the differentiation and classification of land cover types based on their distinct physical attributes and characteristics.

Table 4.2: Biophysical Table

Description	Shade	Kc	Albedo	Green_area	building_intensity
Trees	1	1	0.15	1	0
Buildings	0.2	0.001	0.25	0	0.3
Grass	0	0.95	0.16	1	0
Paved	0	0.001	0.14	0	0.1
Water	0	0.6525	0.09	1	0
Agriculture	0.3	1.22	0.2	1	0
Vacant Land	0	0.001	0.27	0	0

Source: (Author, 2024)

4.5 DATA FOR EVAPOTRANSPIRATION

In Pakistan, the evapotranspiration rate tends to be higher during the warmer seasons, particularly in spring and summer. This increased rate is primarily driven by elevated temperatures and higher solar radiation levels during these seasons. Spring typically experiences rising temperatures as the region transitions from winter to summer, leading to increased evaporation from surfaces and transpiration from plants. During summer, Pakistan often encounters intense heatwaves and prolonged periods of high temperatures, further exacerbating evapotranspiration rates. Additionally, lower humidity levels prevalent during these seasons contribute to greater evaporation rates.

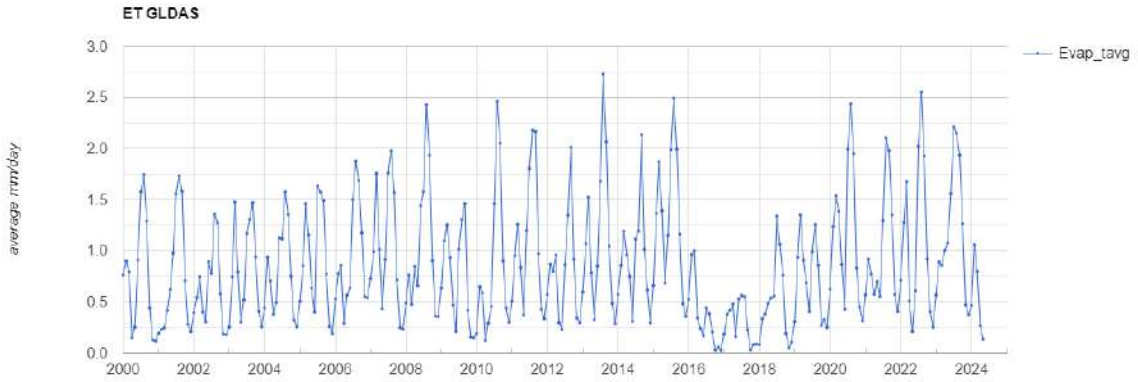

Figure 4.5: Average Evapotranspiration since Last 24 Years for AOI (Author, 2024)

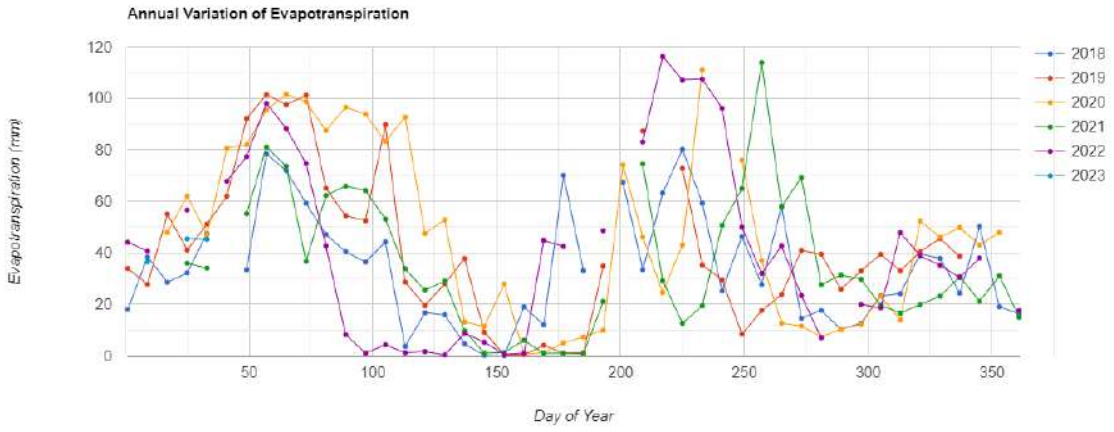

Figure 4.6: Annual Variations in Evapotranspiration Rates for AOI (Author, 2024)

4.6 LAND SURFACE TEMPERATURE AND UHI

With land surface temperatures ranging from 32.0 to 53.5 degrees Celsius and UHI values spanning from -3.0 to 3.8 degrees Celsius, and this align with the expected temperature variations and UHI effects observed during the hot weather conditions of Lahore.

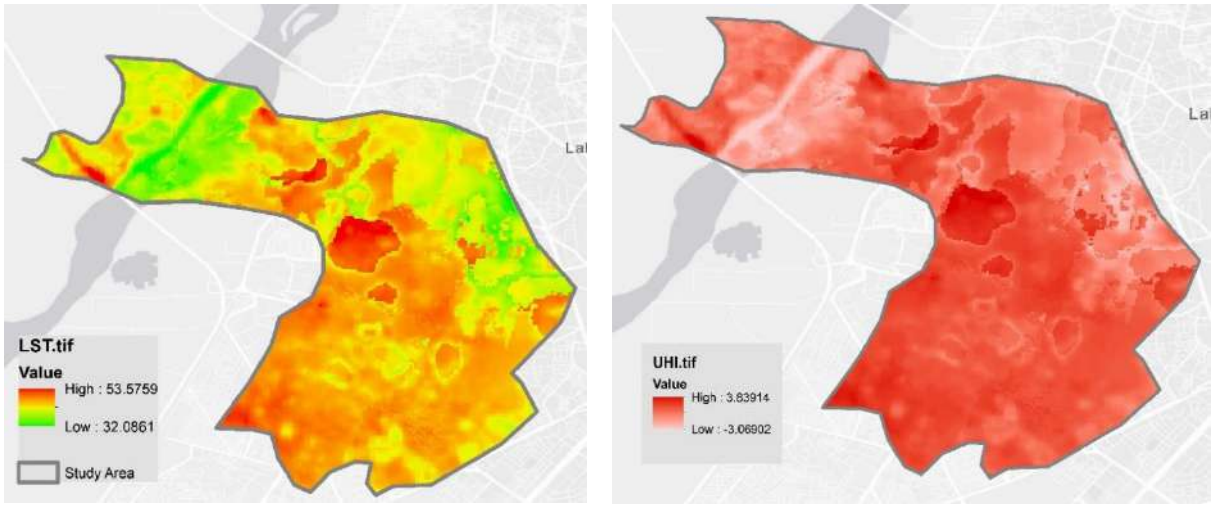

Land Surface Temperatures *UHI*

Figure 4.7: Land Surface Temperature and UHI (Author, 2024)

4.7 OUPUT MAPS FROM BIOPHYSICAL TABLE

The InVEST UCM generates spatial representations of green area, albedo, Kc, and shade. They are included in the appendix section of the report for reference and further analysis.

4.8 BUILDING FOOTPRINT

The building footprints map generated from the GEE was categorized into three different confidentiality levels as given in the figure down below. Notably, areas with a confidentiality level exceeding 0.75 were greater in number. Very less development is seen on the western side of the study area. This vector map is also highlighting the development patterns and road layouts within AOI.

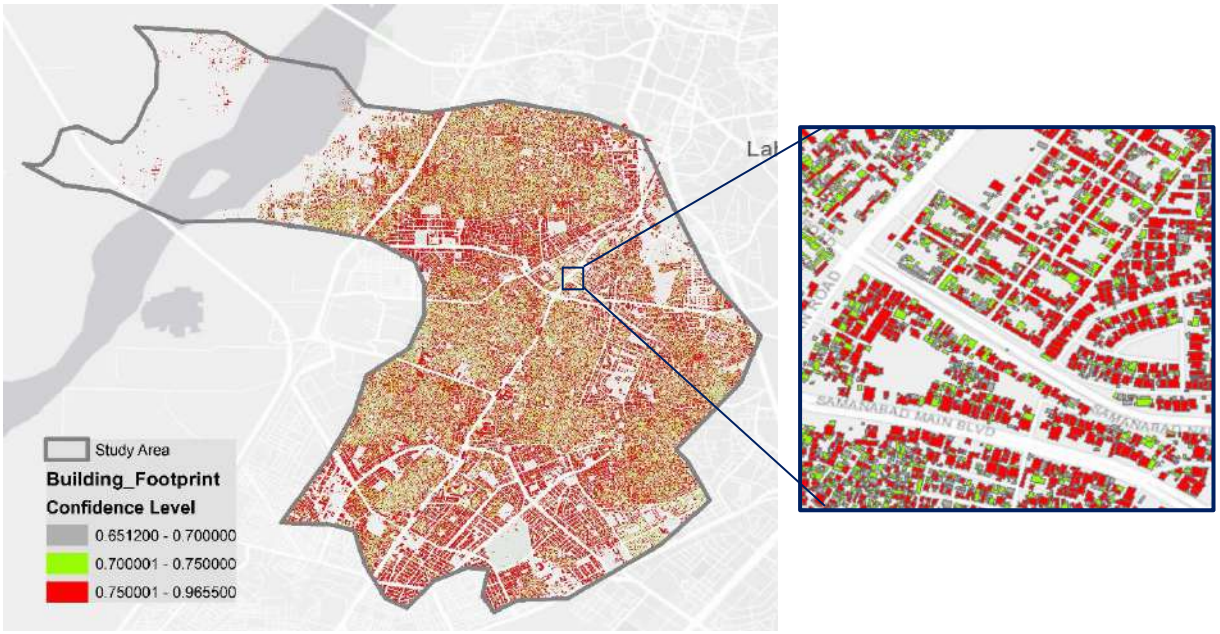

Figure 4.8: Building Footprint (Author, 2024)

4.9 COOLING CAPACITY

The output from the UCM offers insights into the thermal comfort gradient across the city, revealing how it varies from the outskirts to the urban core. This visualization illustrates areas with higher CC levels, depicted by darker shades of blue transitioning to lower levels in yellow. The CC map derived from the InVEST UCM offers valuable insights into how parks contribute to moderating urban heat. It quantifies the extent to which these green spaces help reduce temperatures, providing crucial information for urban planning and management.

Parks with higher cooling capacities serve as vital components of urban green infrastructure, fostering more comfortable environments and potentially mitigating the adverse effects of heat stress on residents. This analysis helps in identifying areas where investments in green spaces can yield maximum cooling benefits, enhancing urban resilience to climate change.

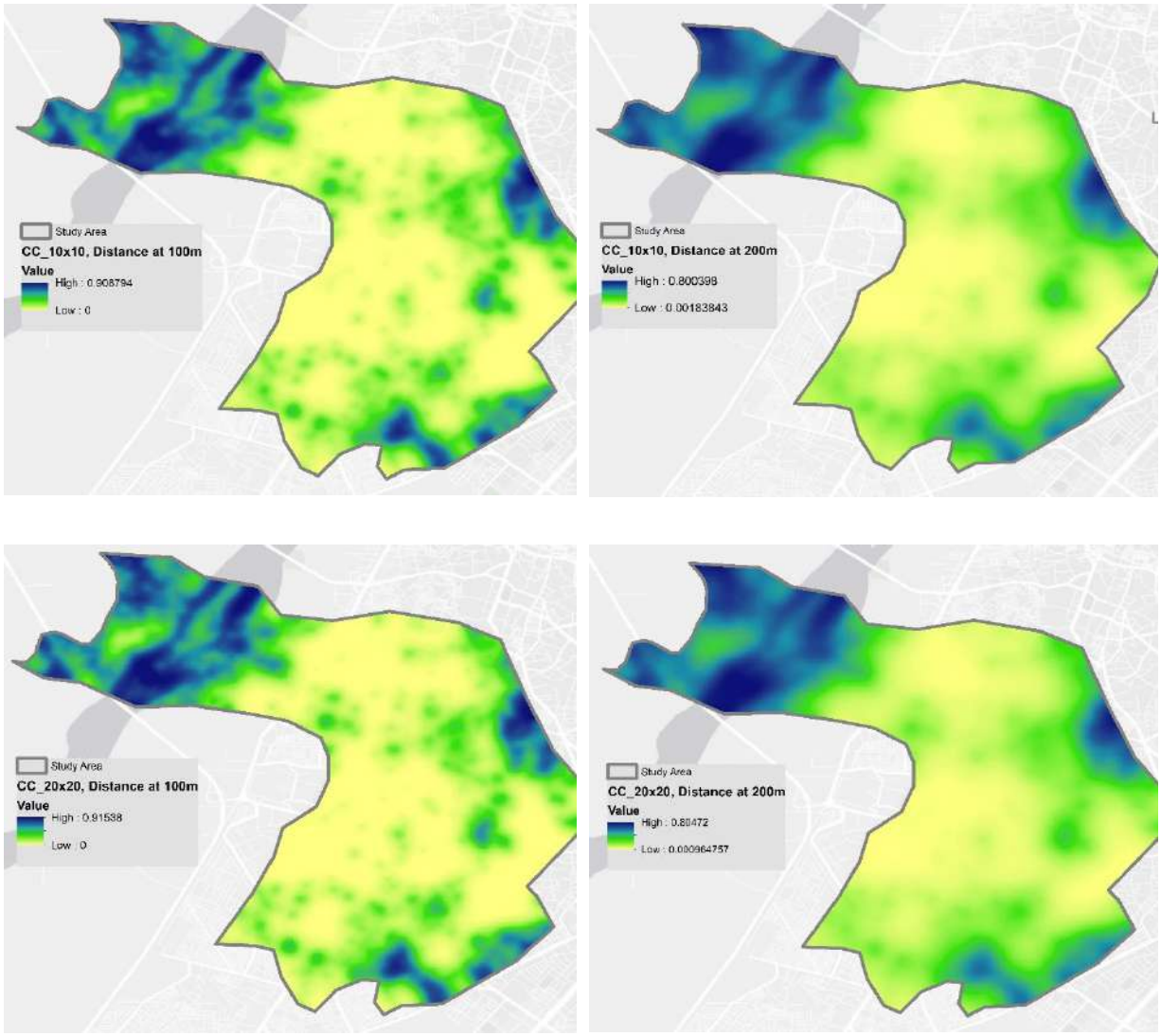

Figure 4.9: Cooling Capacity of Parks and Water Bodies (Author, 2024)

4.10 HEAT MITIGATION INDEX

The heat mitigation index maps generated by the InVEST UCM at cooling distances of 100 meters and 200 meters provide insights into the spatial distribution of cooling within the built environment. Comparatively, the map generated at a cooling distance of 200 meters tends to exhibit a higher spread, indicating a broader coverage of cooling effects. This suggests that at a distance of 200 meters from green spaces, the cooling influence extends further into the surrounding built-up areas, potentially offering more significant cooling benefits to the urban environment compared to the 100-meter distance.

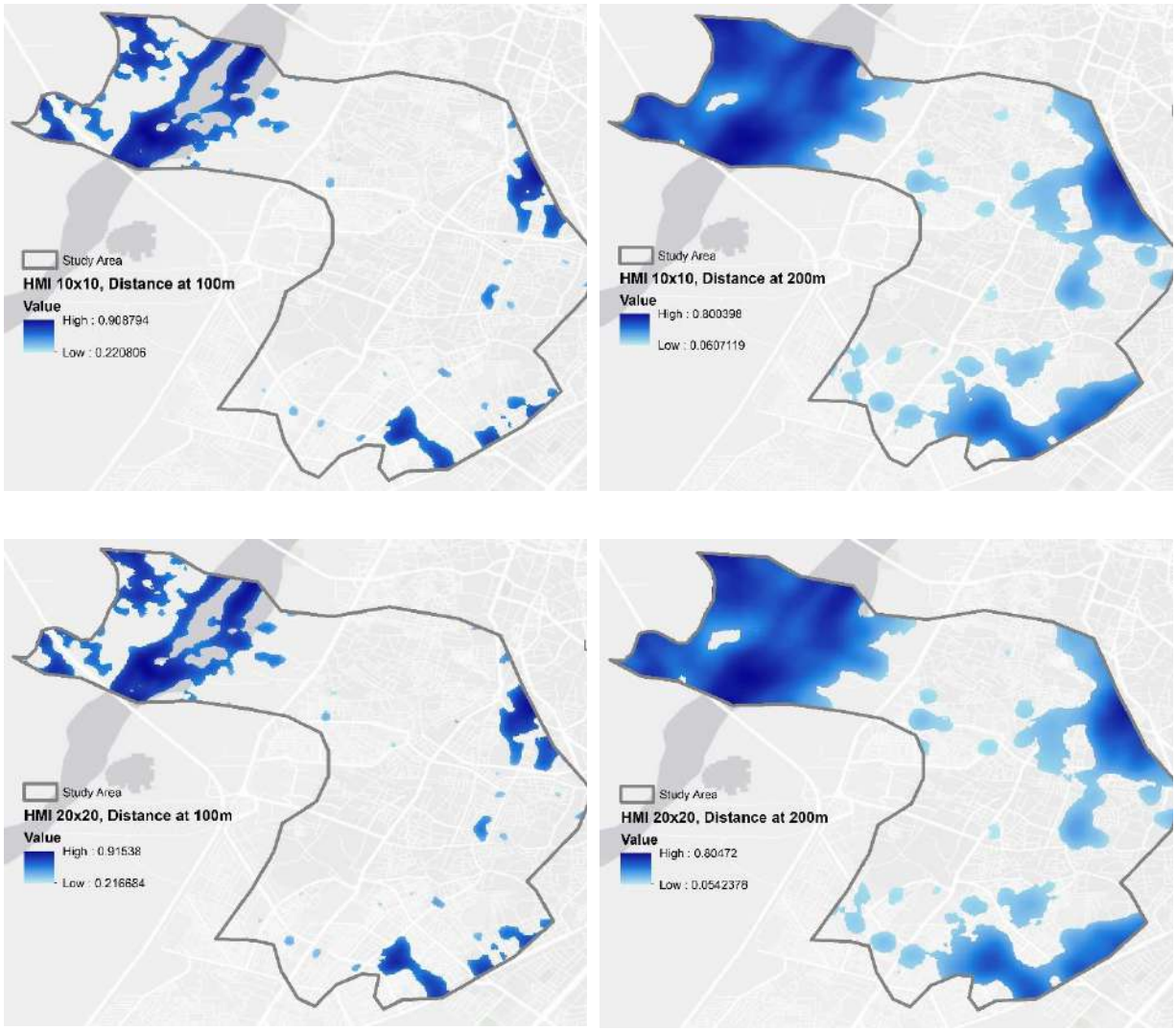

Figure 4.10: Heat Mitigation Index at Different Resolutions and Two Different Cooling Distances (Author, 2024)

5 DISCUSSION AND ANALYSIS

This section involves the detailed analysis of the relationship between CC of large green spaces and the LST. Further it goes deeper and breakdown the analysis to the level of separate LULC categories.

5.1 REGRESSION ANALYSIS BETWEEN LST AND CC

The graphs below represent linear regression models designed to assess the relationship between LST and CC within urban area. The model was provided with the specific spatial resolutions, namely 10 meters and 20 meters, and cooling distances of 100 meters and 200 meters. These four scenarios were generated. In each graph, LST serves as the predicted variable, while CC acts as the predictor, reflecting the capacity of green spaces to alleviate heat stress.

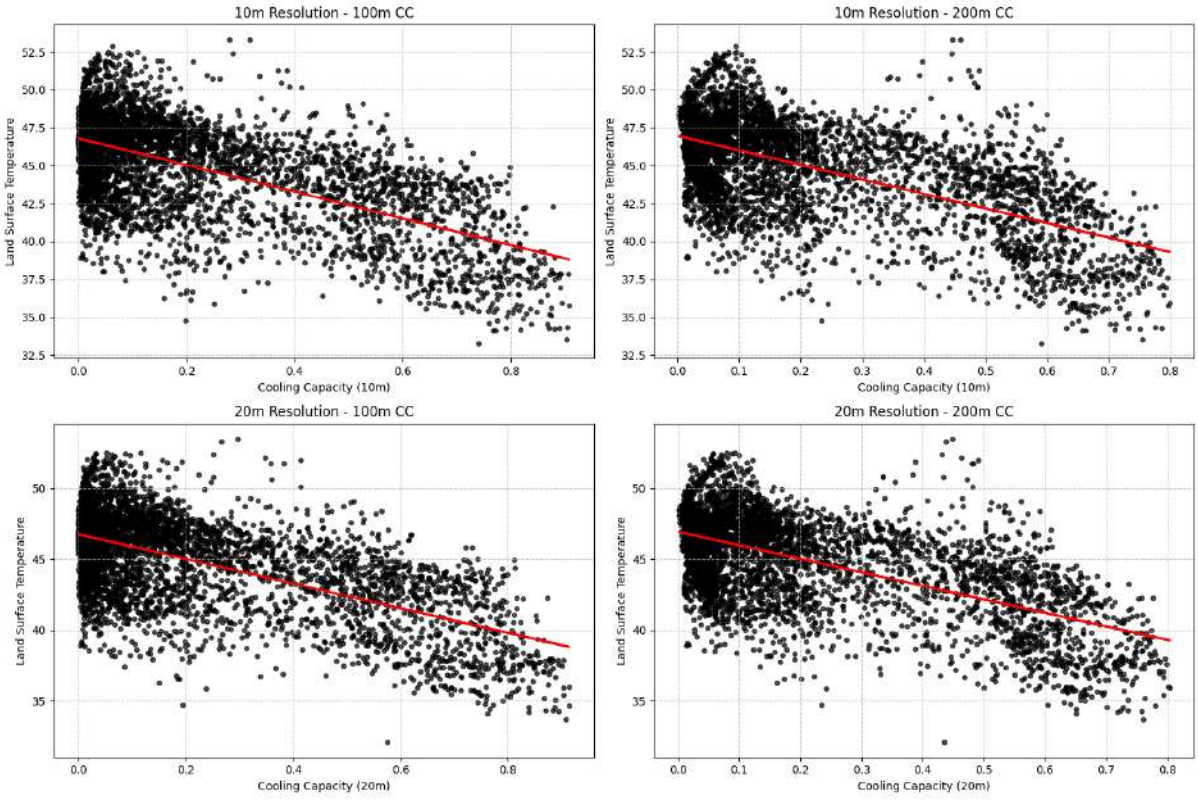

Figure 5.1: Linear Regression between LST and CC for Each Scenario (Author, 2024)

The lien above is showing the inverse relation between two variables. The coefficients accompanying CC in each equation below illustrate the magnitude of change in LST for a unit increase in CC, with negative values indicating an inverse relationship. Additionally, the

intercept terms denote the expected LST when CC is absent. These equations offer a quantitative framework to understand how variations in CC impact land surface temperatures across different spatial scales and distances, providing valuable insights for urban heat mitigation strategies and planning efforts. Equations for each scenario is given as follow:

*10m Resolution - 100m CC: LST = 46.79 -8.80 * CC*

*10m Resolution - 200m CC: LST = 46.97 -9.59 * CC*

*20m Resolution - 100m CC: LST = 46.75 -8.70 * CC*

*20m Resolution - 200m CC: LST = 46.94 -9.54 * CC*

This table provides an understanding of the impact of changes in CC on LST within urban areas, considering different scenarios based on spatial resolution and cooling distance. Negative values indicate that as CC increases, LST tends to decrease, indicating a cooling effect. The "Standard Deviation of Change in LST" column indicates the variability or dispersion in the observed changes in LST across multiple instances or locations within each scenario. A lower standard deviation suggests that changes in LST are more consistent and predictable within the specified scenario.

Table 5.1: Table Showing Change in LST due to 0.1 change in CC

Scenario	Change in LST due to 0.1 change in CC	Standard Deviation of Change in LST
10m_100m	-0.880	0.04400
10m_200m	-0.959	0.05754
20m_100m	-0.870	0.03480
20m_200m	-0.954	0.06678

Source: (Author, 2024)

5.2 ASSESSMENT WITHIN INDIVIDUAL LC TYPES

In the provided scenarios, we observe negative values for the change in Land Surface Temperature (LST) with respect to a 0.1 change in CC across various land cover types. This negative change suggests that an increase in CC is associated with a decrease in land surface temperature.

CC is a measure of the ability of a surface to dissipate heat, and higher CC values indicate better heat dissipation, which leads to lower surface temperatures. Conversely, lower CC values suggest reduced heat dissipation, resulting in higher surface temperatures. Therefore, an increase in CC, such as due to factors like vegetation coverage or water bodies, tends to lower the temperatures and thus this provides us our chance of improvements.

Here are the details for each land cover and land use type and how CC and LST are varying across each.

LULC Class: Trees

R-squared for 10m Resolution (100m CC): 0.3720

R-squared for 10m Resolution (200m CC): 0.3720

R-squared for 20m Resolution (100m CC): 0.321

R-squared for 20m Resolution (200m CC): 0.321

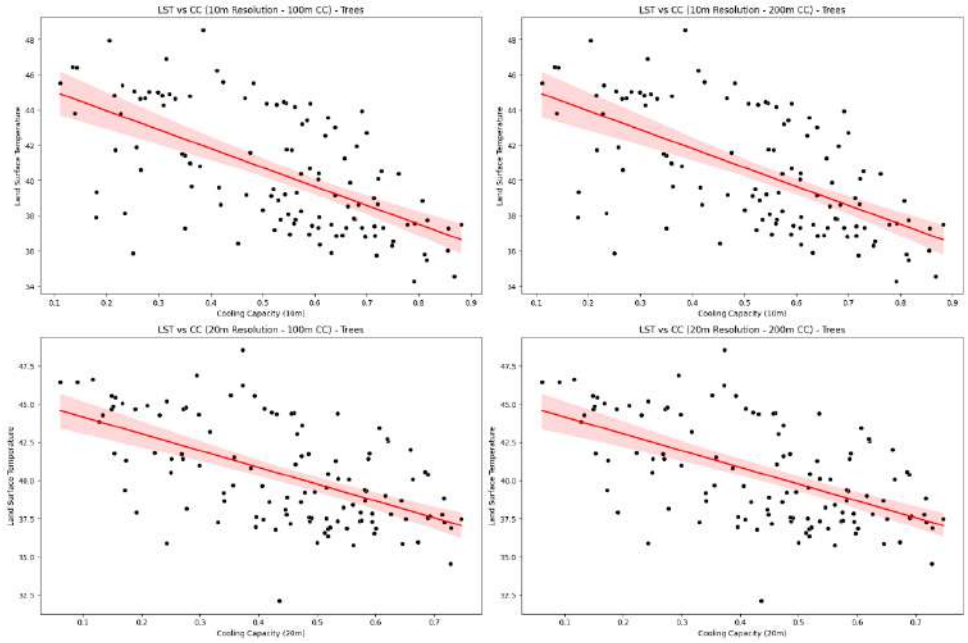

Figure 5.2: Graph for Relationship of LST AND CC among Trees (Author, 2024)

LULC Class: Buildings

R-squared for 10m Resolution (100m CC): 0.057

R-squared for 10m Resolution (200m CC): 0.057

R-squared for 20m Resolution (100m CC): 0.050

R-squared for 20m Resolution (200m CC): 0.050

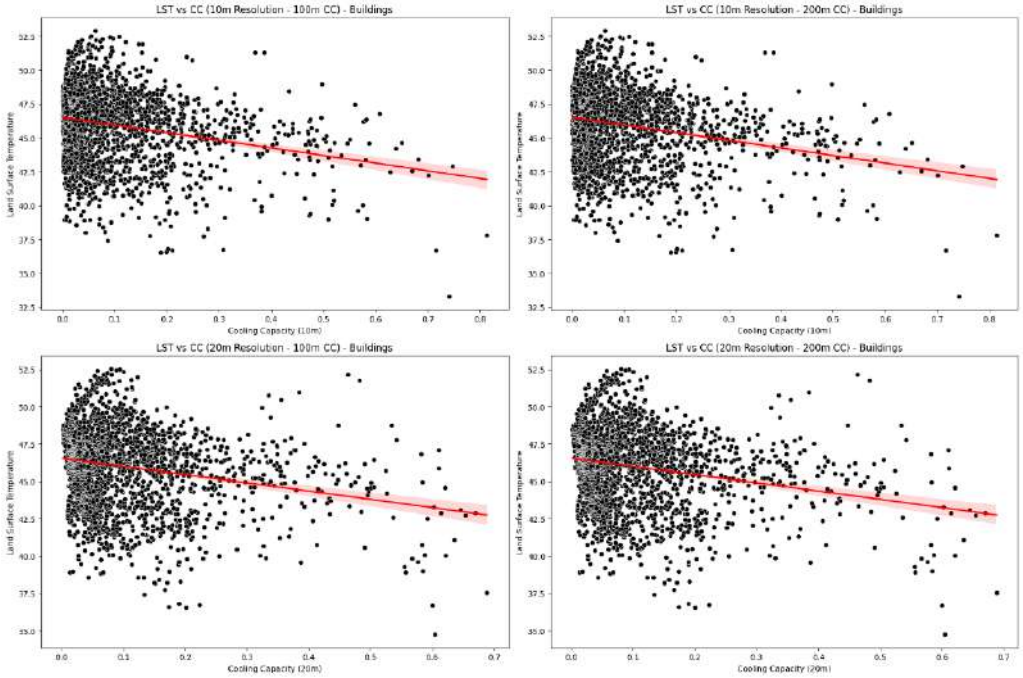

Figure 5.3: Graph for Relationship of LST AND CC among Buildings (Author, 2024)

LULC Class: Grass

R-squared for 10m Resolution (100m CC): 0.2336

R-squared for 10m Resolution (200m CC): 0.2336

R-squared for 20m Resolution (100m CC): 0.2215

R-squared for 20m Resolution (200m CC): 0.2215

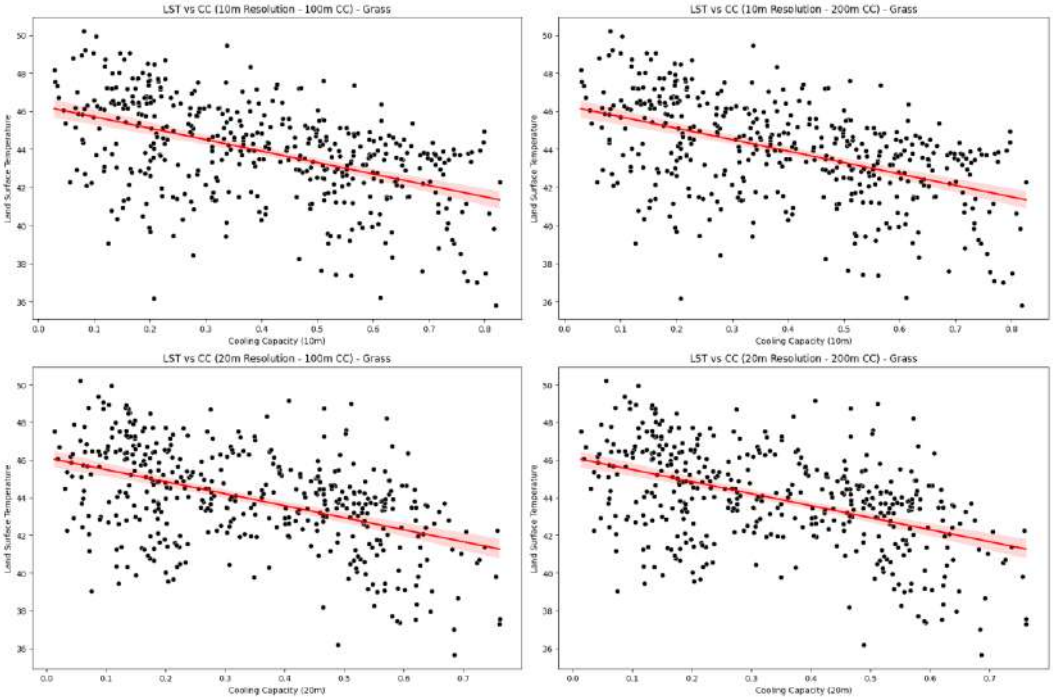

Figure 5.4: Graph for Relationship of LST AND CC among Grass (Author, 2024)

LULC Class: Paved

R-squared for 10m Resolution (100m CC): 0.21501139731121588

R-squared for 10m Resolution (200m CC): 0.21501139731121588

R-squared for 20m Resolution (100m CC): 0.1920448203765247

R-squared for 20m Resolution (200m CC): 0.1920448203765247

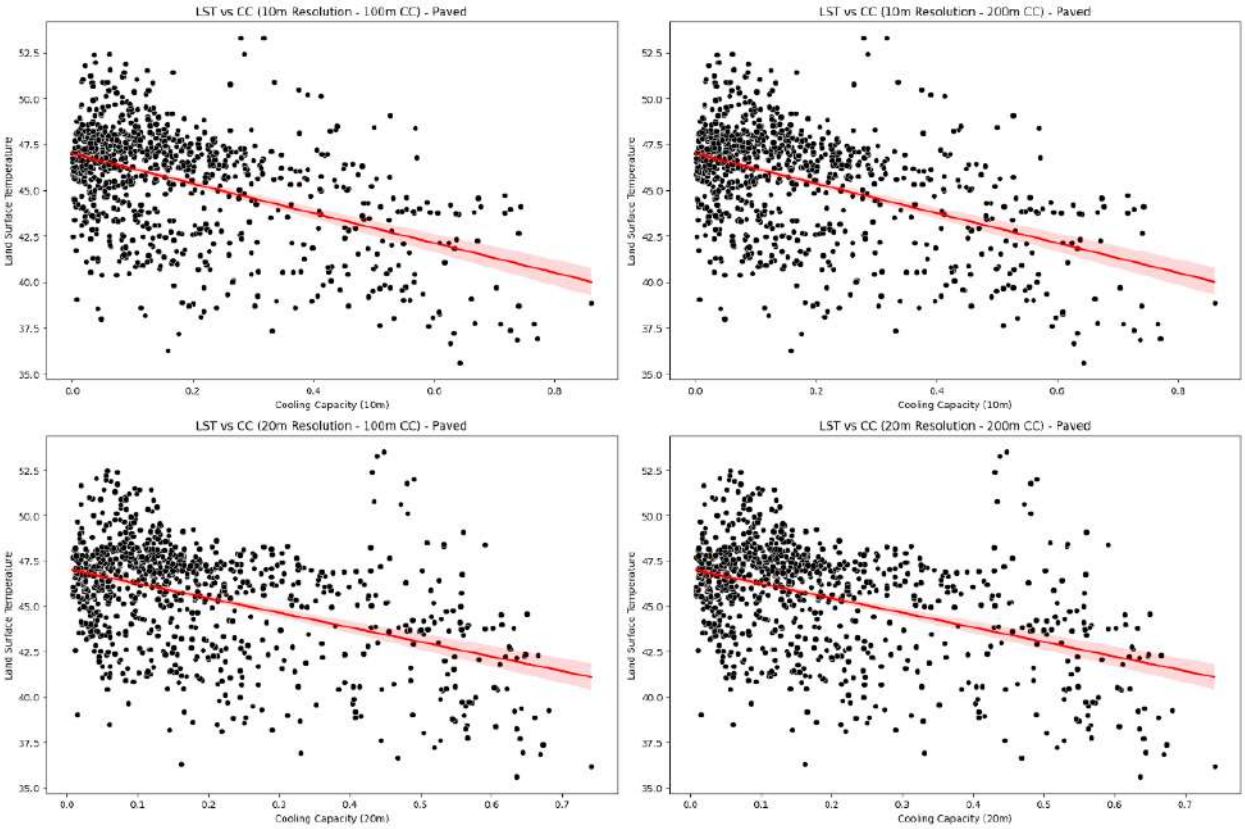

Figure 5.5: Graph for Relationship of LST AND CC among Paved (Author, 2024)

LULC Class: Water

R-squared for 10m Resolution (100m CC): 0.4942

R-squared for 10m Resolution (200m CC): 0.4942

R-squared for 20m Resolution (100m CC): 0.42520

R-squared for 20m Resolution (200m CC): 0.42520

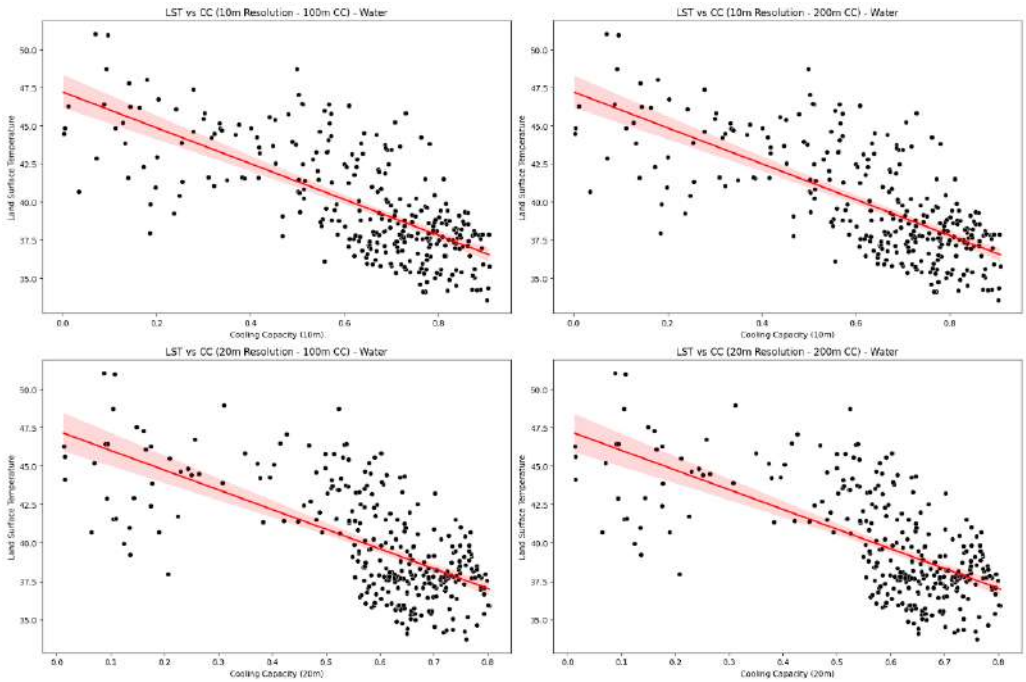

Figure 5.6: Graph for Relationship Of LST And CC among Water (Author, 2024)

LULC Class: Agriculture

R-squared for 10m Resolution (100m CC): 0.0145

R-squared for 10m Resolution (200m CC): 0.0145

R-squared for 20m Resolution (100m CC): 0.0272

R-squared for 20m Resolution (200m CC): 0.0272

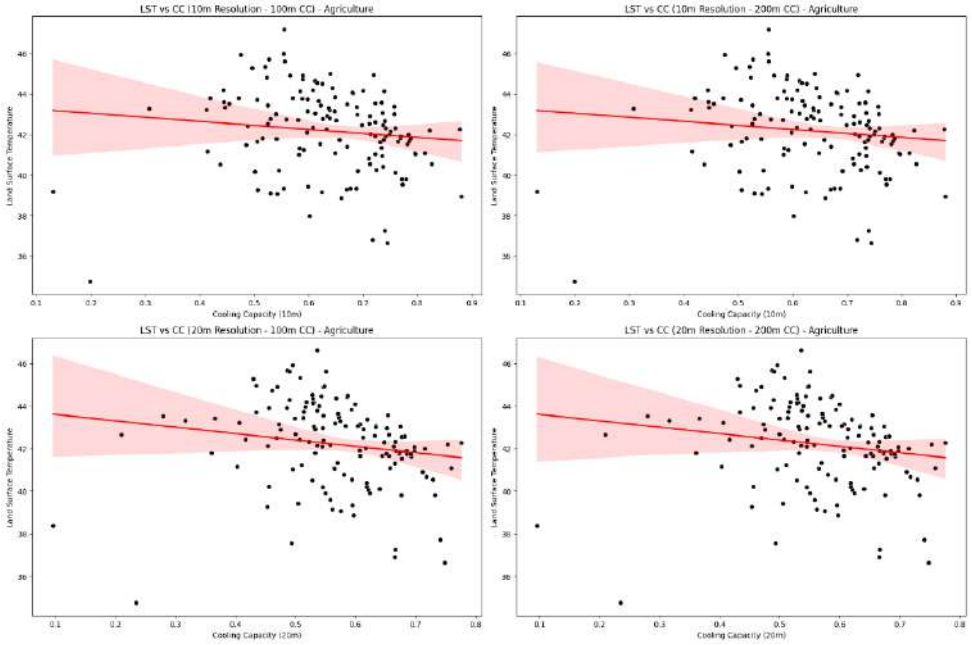

Figure 5.7: Graph for Relationship Of LST And CC among Agriculture (Author, 2024)

LULC Class: Vacant Land

R-squared for 10m Resolution (100m CC): 0.2080682289058433

R-squared for 10m Resolution (200m CC): 0.2080682289058433

R-squared for 20m Resolution (100m CC): 0.2488459616097859

R-squared for 20m Resolution (200m CC): 0.2488459616097859

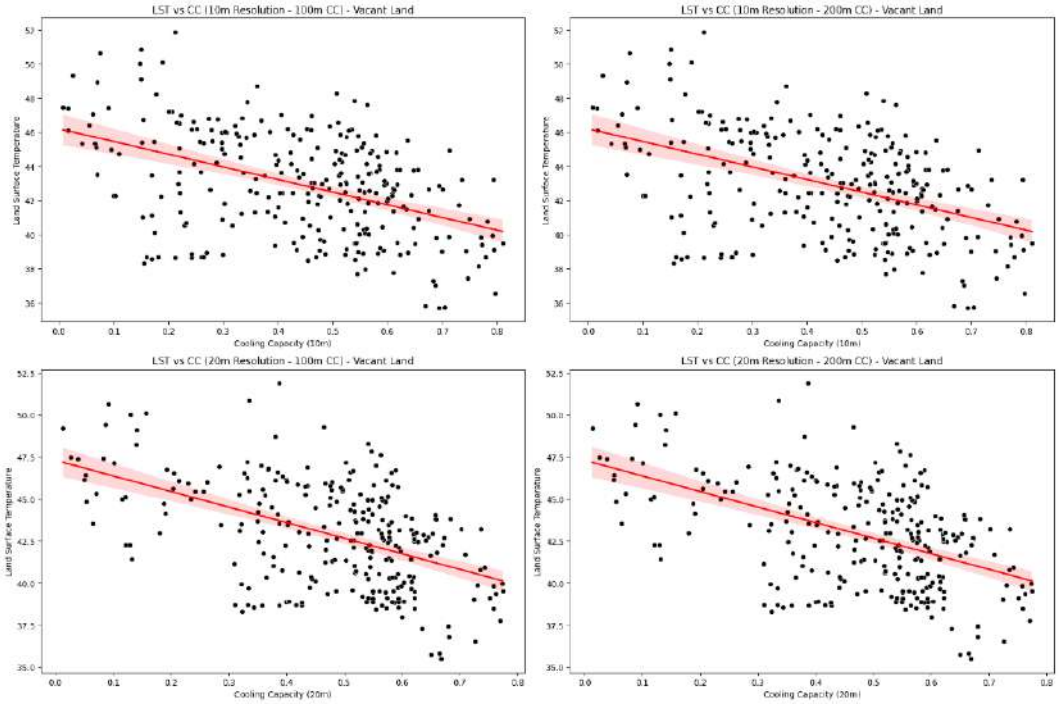

Figure 5.8: Graph for Relationship Of LST And CC among Vacant Land (Author, 2024)

The magnitude of the change varies across different land cover types, which can be attributed to their distinct thermal properties and responses to changes in CC. For example, water bodies typically have higher cooling capacities compared to built-up areas like buildings or paved surfaces. Hence, the change in LST for water bodies tends to be more pronounced compared to other land cover types. Similarly, vegetated areas like trees or grasslands may exhibit varying degrees of change in LST depending on factors such as vegetation density, moisture content, and canopy cover.

Furthermore, the standard deviation values provide insights into the variability or dispersion of the LST data around the predicted values. Higher standard deviation values indicate greater variability in LST within each land cover type, reflecting the heterogeneous nature of surface temperature distributions influenced by factors beyond CC alone.

Table 5.2: Standard deviation and change in LST across each LULC class

Scenario	LULC Class	Change in LST with 0.1 unit change in CC	Std Deviation
10m_100m	Trees	-1.07	2.70
	Buildings	-0.56	2.53
	Grass	-0.60	2.26
	Paved	-0.81	2.71
	Water	-1.18	2.51
	Agriculture	-0.20	2.02
	Vacant Land	-0.74	2.73
10m_200m	Trees	-1.21	2.74
	Buildings	-0.56	2.54
	Grass	-0.64	2.28
	Paved	-0.80	2.76
	Water	-1.31	2.66
	Agriculture	-0.34	2.00
	Vacant Land	-0.94	2.65
20m_100m	Trees	-0.97	2.92
	Buildings	-0.49	2.53
	Grass	-0.50	2.16
	Paved	-0.87	2.65
	Water	-1.27	2.49
	Agriculture	-0.35	1.71
	Vacant Land	-0.64	2.74
20m_200m	Trees	-1.11	2.95
	Buildings	-0.47	2.54
	Grass	-0.52	2.19
	Paved	-0.88	2.68
	Water	-1.48	2.58
	Agriculture	-0.53	1.68
	Vacant Land	-0.90	2.62

Source: (Author, 2024)

In summary, the negative changes in LST and their variations across different land cover types and scenarios underscore the complex interplay between CC, land surface characteristics, and environmental factors influencing surface temperature dynamics. Understanding these relationships is crucial for effective land use planning, climate change mitigation, and UHI management strategies.

The R-squared values provided for each land cover class and resolution scenario represent the goodness of fit of the linear regression model applied to the relationship between LST and

CC. A higher R-squared value indicates that the model explains a greater proportion of the variability in LST based on CC, while lower R-squared values suggest less explanatory power.

Upon analyzing the provided R-squared values, we observe variations across different land cover classes and resolution scenarios. Here are some insights and implications:

5.2.1 Variations among Land Cover Classes

The R-squared values vary among different land cover classes, indicating that the relationship between LST and CC differs depending on land cover characteristics.

For example, water bodies exhibit higher R-squared values compared to other land cover types, suggesting a stronger relationship between CC and LST for water surfaces. This is expected as water bodies have higher thermal inertia and can efficiently dissipate heat, leading to a more pronounced influence on surface temperature.

Conversely, land cover classes like buildings or agriculture may show lower R-squared values, indicating a weaker relationship between CC and LST due to factors such as building materials, land management practices, and vegetation dynamics.

5.2.2 Effect of Resolution

The R-squared values also vary with resolution, indicating the impact of spatial resolution on the relationship between LST and CC.

In general, higher spatial resolutions tend to provide more detailed information, potentially leading to stronger relationships between LST and CC. However, this do not hold true for all land cover classes, as factors such as heterogeneity, scale, and surface characteristics can influence the observed patterns.

Table 5.3: R square values for each land use category

LandUse_Class	**Resolution**	**R-squared for 100m Cooling Distance**	**R-squared for 200m Cooling Distance**
Trees	10px	0.372	0.371

	20px	0.321	0.321
Buildings	10px	0.058	0.058
	20px	0.050	0.051
Grass	10px	0.234	0.235
	20px	0.218	0.222
Paved	10px	0.215	0.218
	20px	0.188	0.192
Water	10px	0.494	0.498
	20px	0.419	0.425
Agriculture	10px	0.015	0.018
	20px	0.023	0.027
Vacant Land	10px	0.208	0.203
	20px	0.249	0.249

Source: (Author, 2024)

5.2.3 Interpretation and Implications

Higher R-squared values suggest that the linear regression model captures a larger proportion of the variability in LST attributed to CC, indicating a better fit of the model to the data.

Lower R-squared values imply that other factors not included in the model may contribute significantly to the variability in LST. These factors could include atmospheric conditions, topography, land use patterns, and anthropogenic influences.

Understanding the variations in R-squared values across different land cover classes and resolutions is crucial for interpreting the results accurately and designing effective land management and climate adaptation strategies.

It's important to consider the limitations of the linear regression approach and explore more complex modeling techniques to account for the multifaceted nature of land surface temperature dynamics.

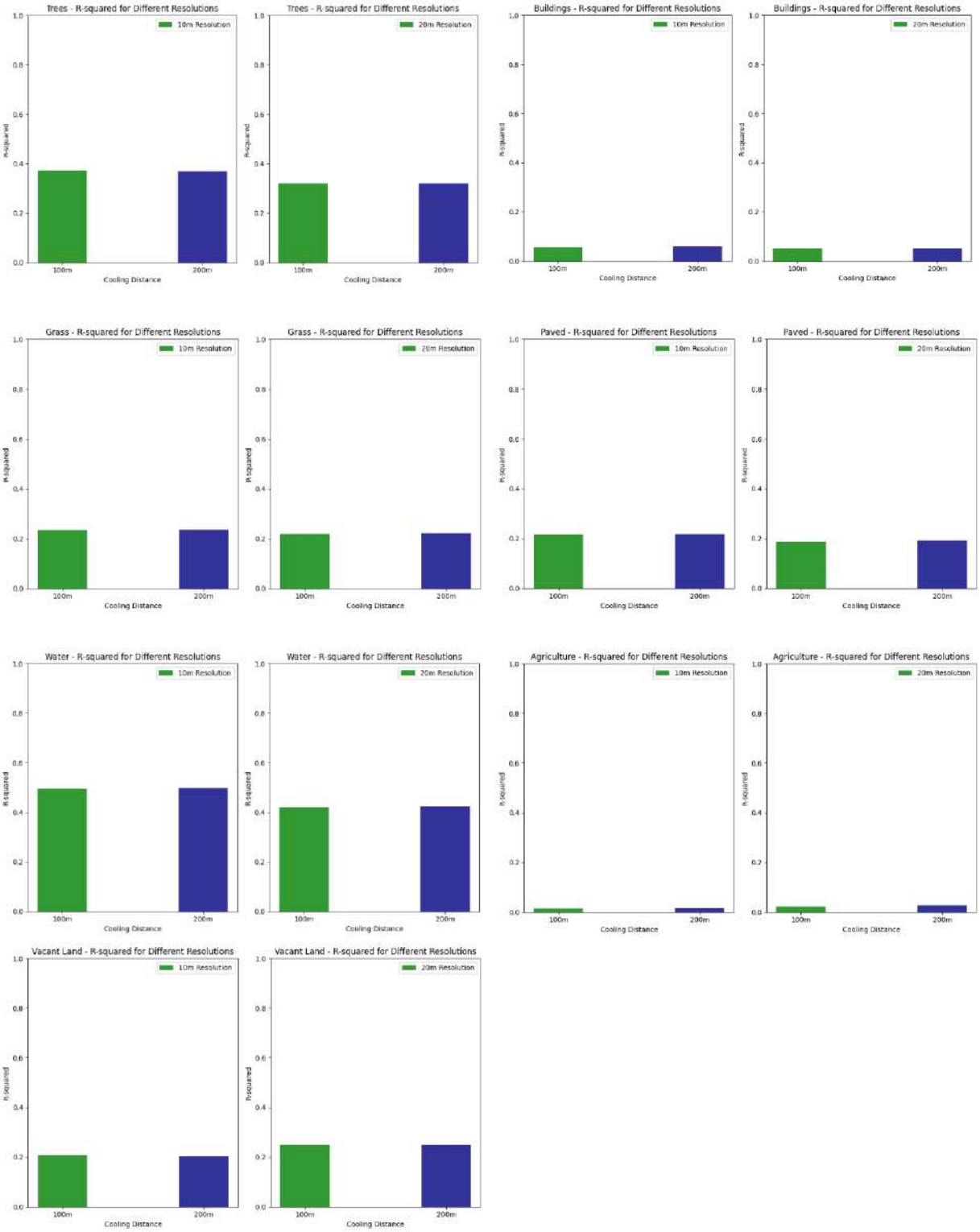

Figure 5.9: Bar Graph showing R square values for each LULC Class (Author, 2024)

6 CONCLUSIONS AND RECOMMENDATIONS

This section presents the summary of the key findings gained from the analysis conducted. In this part, we drew conclusions based on the results presented in the preceding sections, highlighting the significance of our findings and presenting their implications for the real-world implementation.

6.1 CONCLUSIONS

As the risks posed by urban heat extremes continue to rise, it is imperative for cities to formulate strategies aimed at mitigating heat exposure. Consequently, comprehending the differential heat exposure encountered by various communities within urban locales, where the built environment exacerbates extreme heat, becomes increasingly critical.

The analysis of this study highlights the crucial role of green infrastructure in mitigating urban heat by examining the relationship between CC and LST across various LULC types. The inverse correlation between CC and LST indicates that increasing CC, such as through enhanced vegetation and the integration of water bodies, effectively reduces surface temperatures. This effect is most pronounced in water bodies due to their high thermal inertia, whereas built-up areas like buildings exhibit a weaker correlation, emphasizing the challenge of addressing urban heat in densely constructed environments.

The information provided in this study can serve as an important factor for urban planning decisions and motivate municipalities to engage with city initiatives and incentives aimed at promoting environmental justice. It will also be enhancing the resilience of our urban centers in the face of escalating summer temperatures. Integrating climatic knowledge into planning practices in the Lahore metropolitan area would reduce vulnerability to extreme heat events and mitigate the adverse impacts of rising temperatures on public health.

The values provide in the discussion and analysis section can provide valuable insights into the relationships between LST and CC across various land cover types and resolutions, facilitating informed decision-making in urban planning, environmental management, and climate change mitigation efforts.

6.2 RECOMMENDATIONS

As spatial data availability, scientific knowledge, and practical applications continue to advance, and the demand for accessible urban assessments grows, there's an opportunity to develop a comprehensive, globally applicable approach for assessing natural infrastructure in cities worldwide.

While in Pakistan, our policies represent progress, they often lack specificity for addressing adverse temperature effects at the local level. Moreover, they lack consistency in planning implementation methods and steps for evaluating progress toward reducing UHI effects. They need to understand the whole methodology of implementing some clean green initiative. Such directions are provided by these models and tools developed under the umbrella of research and development.

Apart from rejuvenating brown land and securing inner city areas for green and open spaces, we need to enhance the CC of our existing carbon sinks. That way, these sinks will be working on much better cooling distances. Implementing the sponge city concept in Lahore will be important due to the depleting ground table sand rising UHI levels. Lahore faces significant challenges during the monsoon season, with heavy rainfall overwhelming the inadequate drainage systems, leading to widespread flooding. This not only disrupts daily life but also causes extensive damage to infrastructure and poses health risks.

Additionally, the extensive use of impermeable surfaces like concrete and asphalt in the city amplifies the UHI, resulting in higher temperatures and increased energy consumption for cooling. Parks can be improved by increasing vegetation in urban parks, converting some sealed areas (excluding paths, sports fields, allotments, and cemeteries) into low vegetation spaces and adding a tree for every 100 m2 of plantable area to boost tree coverage (Cortinovis et al., 2022).

Implementing green city principles in Lahore would bring multiple environmental and social benefits. By integrating green infrastructure such as parks, green roofs, and restored wetlands, the city can enhance its resilience to climate change, improve air quality, and improve biodiversity. These measures would not only mitigate flooding and heat stress but also create healthier and more livable urban spaces for residents.

7 AREAS FOR FUTURE RESEARCH

In our InVEST UCM research, the primary focus was on assessing the CC of UGSs. While this provides valuable insights into how green infrastructure can mitigate urban heat, there are several additional parameters and complementary models that can be explored to expand and improve the research, offering a more comprehensive understanding of urban systems.

7.1 ENERGY SAVINGS VALUATION

One potential area is the inclusion of energy savings valuation. By incorporating parameters such as building energy consumption and energy savings, we can quantify the economic benefits of reduced cooling demand in buildings due to lower urban temperatures. This can be achieved by integrating a vector layer of buildings and using an energy consumption table (CSV) to model the energy savings associated with reduced urban temperatures. Running simulations to estimate the reduction in energy consumption for air conditioning in residential and commercial buildings would provide valuable data on the economic impact of urban cooling. This has not been added in the study due to limited data availability.

7.2 WORK PRODUCTIVITY VALUATION

Another aspect is evaluating the impact of urban cooling on work productivity. Higher temperatures can reduce worker productivity, and by mitigating urban heat, green infrastructure can potentially enhance work performance as well a mental health. To include this parameter, data on average relative humidity should be collected to better understand the microclimatic conditions affecting productivity.

7.3 COMPREHENSIVE DATA COLLECTION

Future research should emphasize more detailed and comprehensive data collection, particularly on-ground tree canopy data and measuring their diameter. This can be facilitated through government-led initiatives or collaborations with local municipalities. Such data is crucial for accurate modeling of shade and evapotranspiration effects and enhancing the precision of CC estimates. Detailed tree canopy data would allow for more accurate simulations and better-informed urban planning decisions. If more data will be available, then

the InVEST model can be used in combination with other models to produce better outputs that might be having much fruitful implications.

7.4 EXPLORATION OF OTHER INVEST MODELS

Expanding research to other InVEST models can provide a comprehensive view of urban ecosystem services. Potential models include Annual Water Yield and Seasonal Water Yield to assess the impact of urban cooling infrastructure on water availability and hydrological cycles. The Carbon Storage and Sequestration model can evaluate the carbon sequestration potential of UGS and their role in mitigating climate change. For cities with coastal areas, the Coastal Vulnerability model can help understand the protective benefits of coastal green infrastructure against storm surges and sea-level rise and so on.

8 APPENDIX

Outputs from Biophysical Table

Green Areas 

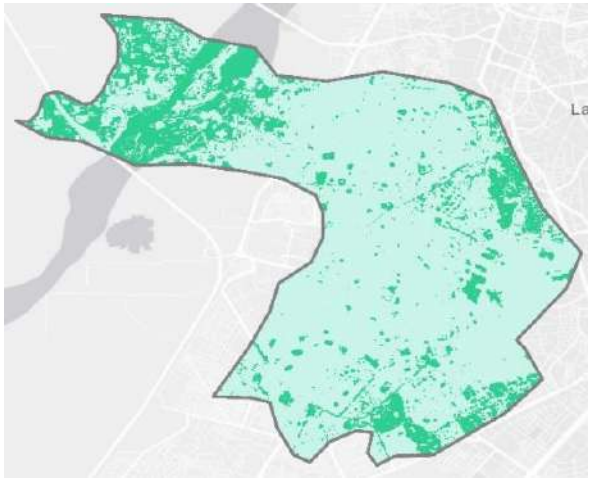

(Resolution at 10m)

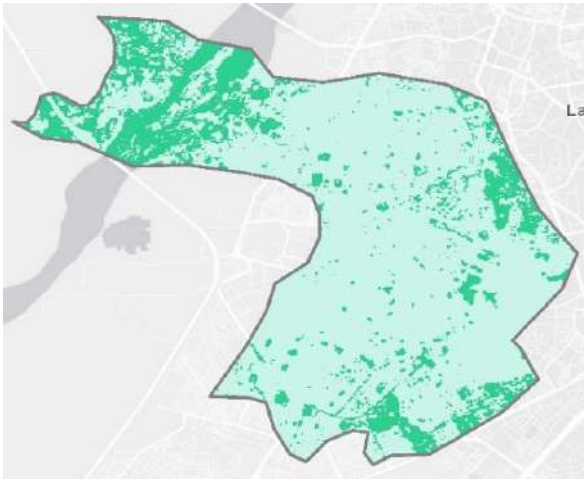

(Resolution at 20m)

Albedo 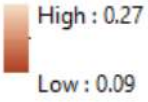

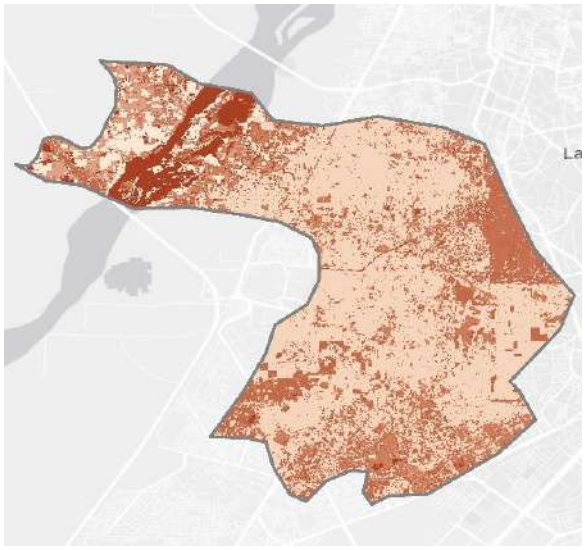

(Resolution at 10m)

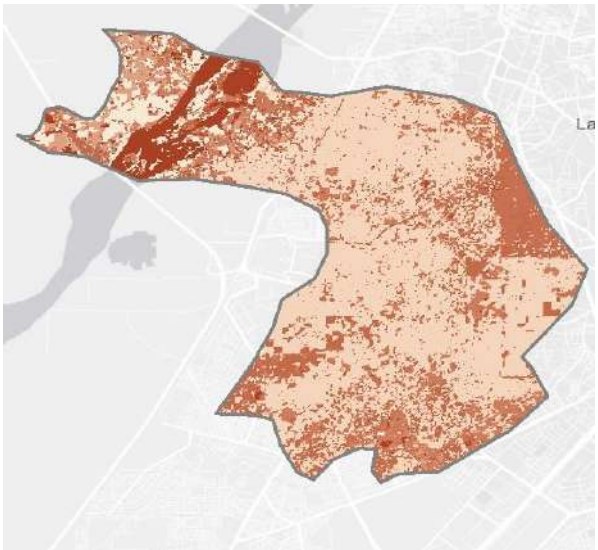

(Resolution at 20m)

Shade

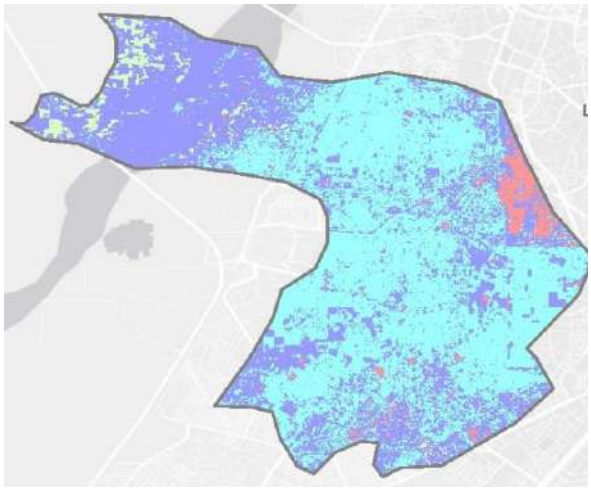

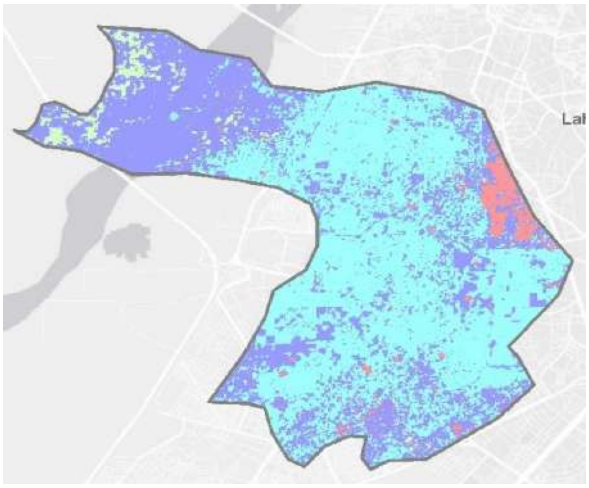

(Resolution at 10m) (Resolution at 20m)

Crop Coefficient (K_c)

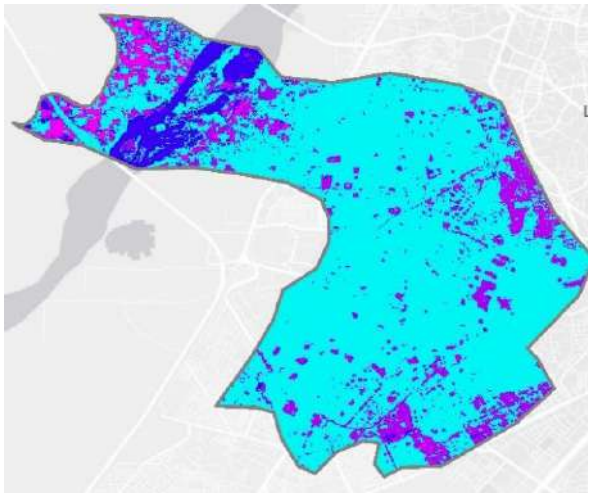

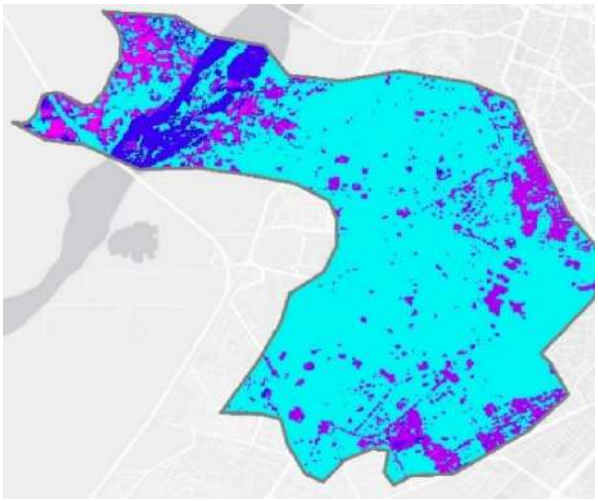

(Resolution at 10m) (Resolution at 20m)

9 BIBLIOGRAPHY

Ahmadi Venhari, A., Tenpierik, M., & Mahdizadeh Hakak, A. (2017). Heat mitigation by greening the cities, a review study. *Environment, Earth and Ecology*, *1*(1), 5–32. https://doi.org/10.24051/eee/67281

Are there real ways to fight climate change? Yes. (n.d.). Retrieved June 7, 2024, from https://www.nationalgeographic.com/environment/article/global-warming-solutions

Arshad, A., Ashraf, M., Sundari, R. S., Qamar, H., Wajid, M., & Hasan, M. (2020). Vulnerability assessment of urban expansion and modelling green spaces to build heat waves risk resiliency in Karachi. *International Journal of Disaster Risk Reduction*, *46*, 101468. https://doi.org/https://doi.org/10.1016/j.ijdrr.2019.101468

Arshad, S., Ahmad, S. R., Abbas, S., Asharf, A., Siddiqui, N. A., & Islam, Z. ul. (2022). Quantifying the contribution of diminishing green spaces and urban sprawl to urban heat island effect in a rapidly urbanizing metropolitan city of Pakistan. *Land Use Policy*, *113*, 105874. https://doi.org/https://doi.org/10.1016/j.landusepol.2021.105874

Artificial Intelligence Forecasting Remote Sensing — QGIS Python Plugins Repository. (n.d.). Retrieved June 3, 2024, from https://plugins.qgis.org/plugins/artificial_intelligence_forecasting_remote_sensing/

Bartesaghi Koc, C., Osmond, P., & Peters, A. (2018). Evaluating the cooling effects of green infrastructure: A systematic review of methods, indicators and data sources. *Solar Energy*, *166*, 486–508. https://doi.org/https://doi.org/10.1016/j.solener.2018.03.008

Battisti, L., Giacco, G., Moraca, M., Pettenati, G., Dansero, E., & Larcher, F. (2024). Spatializing Urban Forests as Nature-based Solutions: a methodological proposal. *Cities*, *144*, 104629. https://doi.org/https://doi.org/10.1016/j.cities.2023.104629

Bornstein, R. D. (1975). The Two-Dimensional URBMET Urban Boundary Layer Model. *Journal of Applied Meteorology and Climatology*, *14*(8), 1459–1477. https://doi.org/https://doi.org/10.1175/1520-0450(1975)014<1459:TTDUUB>2.0.CO;2

Bosch, M., Locatelli, M., Hamel, P., Remme, R. P., Chenal, J., & Joost, S. (2021). A spatially explicit approach to simulate urban heat mitigation with InVEST (v3.8.0). *Geoscientific Model Development*, *14*(6), 3521–3537. https://doi.org/10.5194/gmd-14-3521-2021

Burkhard, B., Kandziora, M., Hou, Y., & Müller, F. (2014). Ecosystem service potentials, flows and demands-concepts for spatial localisation, indication and quantification. *Landscape Online*, *34*(1), 1–32. https://doi.org/10.3097/LO.201434

Carrasco-Valencia, L., Vilca-Campana, K., Iruri-Ramos, C., Cárdenas-Pillco, B., Ollero, A., & Chanove-Manrique, A. (2024). Effect of LULC Changes on Annual Water Yield in the Urban Section of the Chili River, Arequipa, Using the InVEST Model. *Water*, *16*(5). https://doi.org/10.3390/w16050664

Chen, J., Jönsson, Per., Tamura, M., Gu, Z., Matsushita, B., & Eklundh, L. (2004). A simple method for reconstructing a high-quality NDVI time-series data set based on the Savitzky–Golay filter. *Remote Sensing of Environment*, *91*(3), 332–344. https://doi.org/https://doi.org/10.1016/j.rse.2004.03.014

Chen, X. L., Zhao, H. M., Li, P. X., & Yin, Z. Y. (2006). Remote sensing image-based analysis of the relationship between urban heat island and land use/cover changes. *Remote Sensing of Environment*, *104*(2), 133–146. https://doi.org/10.1016/j.rse.2005.11.016

Cortinovis, C., Olsson, P., Boke-Olén, N., & Hedlund, K. (2022). Scaling up nature-based solutions for climate-change adaptation: Potential and benefits in three European cities. *Urban Forestry & Urban Greening*, *67*, 127450. https://doi.org/https://doi.org/10.1016/j.ufug.2021.127450

de Bont, J., Nori-Sarma, A., Stafoggia, M., Banerjee, T., Ingole, V., Jaganathan, S., Mandal, S., Rajiva, A., Krishna, B., Kloog, I., Lane, K., Mall, R. K., Tiwari, A., Wei, Y., Wellenius, G. A., Prabhakaran, D., Schwartz, J., Prabhakaran, P., & Ljungman, P. (2024). Impact of heatwaves on all-cause mortality in India: A comprehensive multi-city study. *Environment International*, *184*, 108461. https://doi.org/https://doi.org/10.1016/j.envint.2024.108461

Dunne, J. P., Stouffer, R. J., & John, J. G. (2013). Reductions in labour capacity from heat stress under climate warming. *Nature Climate Change*, *3*(6), 563–566. https://doi.org/10.1038/nclimate1827

Frantzeskaki, N. (2019). Seven lessons for planning nature-based solutions in cities. *Environmental Science & Policy*, *93*, 101–111. https://doi.org/https://doi.org/10.1016/j.envsci.2018.12.033

Gallay, I., Olah, B., Murtinová, V., & Gallayová, Z. (2023). Quantification of the Cooling Effect and Cooling Distance of Urban Green Spaces Based on Their Vegetation Structure and Size as a Basis for Management Tools for Mitigating Urban Climate. *Sustainability (Switzerland)*, *15*(4). https://doi.org/10.3390/su15043705

Gao, B. (1996). NDWI—A normalized difference water index for remote sensing of vegetation liquid water from space. *Remote Sensing of Environment*, *58*(3), 257–266. https://doi.org/https://doi.org/10.1016/S0034-4257(96)00067-3

Gratani, L., Varone, L., & Bonito, A. (2016). Carbon sequestration of four urban parks in Rome. *Urban Forestry and Urban Greening*, *19*, 184–193. https://doi.org/10.1016/j.ufug.2016.07.007

Green City Case Study: Melbourne, Australia: Grey to Green • AIPH. (n.d.). Retrieved June 6, 2024, from https://aiph.org/green-city-case-studies/melbourne-australia/

Greening the City Project - City of Melbourne. (n.d.). Retrieved June 6, 2024, from https://www.melbourne.vic.gov.au/community/greening-the-city/urban-nature/Pages/greening-the-city-project.aspx

Haaland, C., & van den Bosch, C. K. (2015). Challenges and strategies for urban green-space planning in cities undergoing densification: A review. *Urban Forestry & Urban Greening*, *14*(4), 760–771. https://doi.org/https://doi.org/10.1016/j.ufug.2015.07.009

Hamel, P., Bosch, M., Tardieu, L., Lemonsu, A., de Munck, C., Nootenboom, C., Viguié, V., Lonsdorf, E., Douglass, J. A., & Sharp, R. P. (2023). Calibrating and validating the InVEST urban cooling model: Case studies in France and the United States. *EGUsphere*, *2023*, 1–25. https://doi.org/10.5194/egusphere-2023-928

Hamel, P., Guerry, A. D., Polasky, S., Han, B., Douglass, J. A., Hamann, M., Janke, B., Kuiper, J. J., Levrel, H., Liu, H., Lonsdorf, E., McDonald, R. I., Nootenboom, C., Ouyang, Z., Remme, R. P., Sharp, R. P., Tardieu, L., Viguié, V., Xu, D., … Daily, G. C. (2021). Mapping the benefits of nature in cities with the InVEST software. *Npj Urban Sustainability*, *1*(1), 25. https://doi.org/10.1038/s42949-021-00027-9

Hamilton, S. H., Fu, B., Guillaume, J. H. A., Badham, J., Elsawah, S., Gober, P., Hunt, R. J., Iwanaga, T., Jakeman, A. J., Ames, D. P., Curtis, A., Hill, M. C., Pierce, S. A., & Zare, F. (2019). A framework for characterising and evaluating the effectiveness of environmental modelling. *Environmental Modelling & Software*, *118*, 83–98. https://doi.org/https://doi.org/10.1016/j.envsoft.2019.04.008

Hu, Y., Wang, C., & Li, J. (2023). Assessment of Heat Mitigation Services Provided by Blue and Green Spaces: An Application of the InVEST Urban Cooling Model with Scenario Analysis in Wuhan, China. *Land*, *12*(5). https://doi.org/10.3390/land12050963

Hung, T. Le. (2020). Urban Bare Land Classification Using NDBaI Index Based on Combination of Sentinel 2 MSI and Landsat 8 Multiresolution Images. *VNU Journal of Science: Earth and Environmental Sciences*, *36*(2). https://doi.org/10.25073/2588-1094/vnuees.4537

IPCC — Intergovernmental Panel on Climate Change. (n.d.). Retrieved October 12, 2023, from https://www.ipcc.ch/

i-Tree Tools - Calculate the benefits of trees! (n.d.). Retrieved June 4, 2024, from https://www.itreetools.org/

Jaganmohan, M., Knapp, S., Buchmann, C. M., & Schwarz, N. (2016). The Bigger, the Better? The Influence of Urban Green Space Design on Cooling Effects for Residential Areas. *Journal of Environmental Quality*, *45*(1), 134–145. https://doi.org/10.2134/jeq2015.01.0062

Jamei, E., & Rajagopalan, P. (2017). Urban development and pedestrian thermal comfort in Melbourne. *Solar Energy*, *144*, 681–698. https://doi.org/https://doi.org/10.1016/j.solener.2017.01.023

Jia, P., Chen, C., Zhang, D., Sang, Y., & Zhang, L. (2024). Semantic segmentation of deep learning remote sensing images based on band combination principle: Application in urban planning and land use. *Computer Communications*, *217*, 97–106. https://doi.org/https://doi.org/10.1016/j.comcom.2024.01.032

Kadaverugu, R., Gurav, C., Rai, A., Sharma, A., Matli, C., & Biniwale, R. (n.d.). *Quantification of heat mitigation by urban green spaces using InVEST model-a scenario analysis of Nagpur City, India*. https://doi.org/10.1007/s12517-020-06380-w/Published

Kajosaari, A., Hasanzadeh, K., Fagerholm, N., Nummi, P., Kuusisto-Hjort, P., & Kyttä, M. (2024). Predicting context-sensitive urban green space quality to support urban green infrastructure planning. *Landscape and Urban Planning*, *242*, 104952. https://doi.org/https://doi.org/10.1016/j.landurbplan.2023.104952

Keyes, N., Mclaren, C., Phan, N., Vazquez, D., & Liu, J. (2022). *NASA DEVELOP National Program Virtual Environmental Justice-Milwaukee Milwaukee Urban Development Assessing Climate Vulnerability through the InVEST Model on Urban Cooling in Milwaukee Using NASA Earth Observations*.

Kim, J., Kim, D., Jun, H.-J., & Heo, J.-P. (2024). The detection of residential developments in urban areas: Exploring the potentials of deep-learning algorithms. *Computers, Environment and Urban Systems*, *107*, 102053. https://doi.org/https://doi.org/10.1016/j.compenvurbsys.2023.102053

Kunapo, J., Fletcher, T. D., Ladson, A. R., Cunningham, L., & Burns, M. J. (2018). A spatially explicit framework for climate adaptation. *Urban Water Journal*, *15*(2), 159–166. https://doi.org/10.1080/1573062X.2018.1424216

Lahore Population Density Map PDF | PDF | Lahore | Geomatics. (n.d.). Retrieved June 4, 2024, from https://www.scribd.com/document/453032085/Lahore-Population-Density-Map-pdf

Lee, A. C. K., Jordan, H. C., & Horsley, J. (2015). Value of urban green spaces in promoting healthy living and wellbeing: prospects for planning. *Risk Management and Healthcare Policy*, *8*(null), 131–137. https://doi.org/10.2147/RMHP.S61654

Lima, P. R., Pereira, A. A. M., Chaves, G. de L. D., & Meneguelo, A. P. (2021). Environmental awareness and public perception on carbon capture and storage (CCS) in Brazil. *International Journal of Greenhouse Gas Control*, *111*. https://doi.org/10.1016/j.ijggc.2021.103467

Luo, M., Wu, S., Ngar-Cheung Lau, G., Pei, T., Liu, Z., Wang, X., Ning, G., Chan, T. O., Yang, Y., & Zhang, W. (2024). Anthropogenic forcing has increased the risk of longer-traveling and slower-moving large contiguous heatwaves. *Science Advances*, *10*(13). https://doi.org/10.1126/SCIADV.ADL1598/SUPPL_FILE/SCIADV.ADL1598_SM.PDF

MacLachlan, A., Biggs, E., Roberts, G., & Boruff, B. (2021). Sustainable City Planning: A Data-Driven Approach for Mitigating Urban Heat. *Frontiers in Built Environment*, *6*, 519599. https://doi.org/10.3389/FBUIL.2020.519599/BIBTEX

Marland, G., Pielke, R. A., Apps, M., Avissar, R., Betts, R. A., Davis, K. J., Frumhoff, P. C., Jackson, S. T., Joyce, L. A., Kauppi, P., Katzenberger, J., MacDicken, K. G., Neilson, R. P., Niles, J. O., Niyogi, D. S., Norby, R. J., Pena, N., Sampson, N., & Xue, Y. (2003). The climatic impacts of land surface change and carbon management, and the implications for climate-change mitigation policy. *Climate Policy*, *3*(2), 149–157. https://doi.org/10.3763/cpol.2003.0318

Nice, K. A., Demuzere, M., Coutts, A. M., & Tapper, N. (2024). Present day and future urban cooling enabled by integrated water management. *Frontiers in Sustainable Cities*, *6*. https://doi.org/10.3389/frsc.2024.1337449

Niemelä, J., Saarela, S.-R., Söderman, T., Kopperoinen, L., Yli-Pelkonen, V., Väre, S., & Kotze, D. J. (2010). Using the ecosystem services approach for better planning and conservation of urban green spaces: a Finland case study. *Biodiversity and Conservation*, *19*(11), 3225–3243. https://doi.org/10.1007/s10531-010-9888-8

Onder, S., & Dursun, S. (2010). Global Climate Changes and Effects on Urban Climate of Urban Green Spaces. *International Journal of Thermal and Environmental Engineering*, *3*(1), 37–41. https://doi.org/10.5383/ijtee.03.01.006

Pakistan: From Global Warming To Global Boiling. (n.d.). Retrieved June 6, 2024, from https://thefridaytimes.com/05-Jun-2024/pakistan-from-global-warming-to-global-boiling

Pakistan Population (2024) - Worldometer. (n.d.). Retrieved June 3, 2024, from https://www.worldometers.info/world-population/pakistan-population/

Pakistan Urban Population 1960-2024 | MacroTrends. (n.d.). Retrieved June 3, 2024, from https://www.macrotrends.net/global-metrics/countries/PAK/pakistan/urban-population

Pauleit, S., Hansen, R., Rall, E. L., Zölch, T., Andersson, E., Luz, A. C., Szaraz, L., Tosics, I., & Vierikko, K. (2017). Urban Landscapes and Green Infrastructure. *Oxford Research Encyclopedia of Environmental Science*. https://doi.org/10.1093/ACREFORE/9780199389414.013.23

Phelan, P. E., Kaloush, K., Miner, M., Golden, J., Phelan, B., Silva, H., & Taylor, R. A. (2015). Urban Heat Island: Mechanisms, Implications, and Possible Remedies. *Annual Review of Environment and Resources*, *40*, 285–307. https://doi.org/10.1146/annurev-environ-102014-021155

Practical considerations and challenges to greenspace - Forest Research. (n.d.). Retrieved June 3, 2024, from https://www.forestresearch.gov.uk/tools-and-resources/fthr/urban-regeneration-and-greenspace-partnership/practical-considerations-and-challenges-to-greenspace/

Rauf, S., Bakhsh, K., Abbas, A., Hassan, S., Ali, A., & Kächele, H. (2017). How hard they hit? Perception, adaptation and public health implications of heat waves in urban and peri-urban Pakistan. *Environmental Science and Pollution Research*, *24*(11), 10630–10639. https://doi.org/10.1007/s11356-017-8756-4

Ready-to-Use Geospatial Deep Learning Models. (n.d.). Retrieved June 3, 2024, from https://www.esri.com/about/newsroom/arcuser/deep-learning-models/

Ronchi, S., Salata, S., & Arcidiacono, A. (2020). Which urban design parameters provide climate-proof cities? An application of the Urban Cooling InVEST Model in the city of Milan comparing historical planning morphologies. *Sustainable Cities and Society*, *63*, 102459. https://doi.org/https://doi.org/10.1016/j.scs.2020.102459

Scharfstädt, L., Schöneberger, P., Simon, H., Sinsel, T., Nahtz, T., & Bruse, M. (2024). From Oasis to Desert: The Struggle of Urban Green Spaces Amid Heatwaves and Water Scarcity. *Sustainability 2024, Vol. 16, Page 3373*, *16*(8), 3373. https://doi.org/10.3390/SU16083373

Shaping a Heat Resilient City. (n.d.). Retrieved June 7, 2024, from https://www.ura.gov.sg/Corporate/Get-Involved/Plan-Our-Future-SG/Innovative-Urban-Solutions/Heat-resilient-city

Sidhu, N., Pebesma, E., & Câmara, G. (2018). Using Google Earth Engine to detect land cover change: Singapore as a use case. *European Journal of Remote Sensing*, *51*(1), 486–500. https://doi.org/10.1080/22797254.2018.1451782

Sirakaya, A., Cliquet, A., & Harris, J. (2018). Ecosystem services in cities: Towards the international legal protection of ecosystem services in urban environments. *Ecosystem Services*, *29*, 205–212. https://doi.org/https://doi.org/10.1016/j.ecoser.2017.01.001

Sirko, W., Kashubin, S., Ritter, M., Annkah, A., Bouchareb, Y. S. E., Dauphin, Y., Keysers, D., Neumann, M., Cisse, M., & Quinn, J. (2021). *Continental-Scale Building Detection from High Resolution Satellite Imagery*. https://sites.research.google/open-buildings/

Solving Singapore's urban heat island effect. (n.d.). Retrieved June 7, 2024, from https://phys.org/news/2024-02-singapore-urban-island-effect.html

Sun, Y., Ilango, S. D., Schwarz, L., Wang, Q., Chen, J. C., Lawrence, J. M., Wu, J., & Benmarhnia, T. (2020). Examining the joint effects of heatwaves, air pollution, and green space on the risk of preterm birth in California. *Environmental Research Letters*, *15*(10), 104099. https://doi.org/10.1088/1748-9326/ABB8A3

Sun, Y., Zhu, S., Wang, D., Duan, J., Lu, H., Yin, H., Tan, C., Zhang, L., Zhao, M., Cai, W., Wang, Y., Hu, Y., Tao, S., & Guan, D. (2024). Global supply chains amplify economic costs of future extreme heat risk. *Nature*, *627*(8005), 797–804. https://doi.org/10.1038/s41586-024-07147-z

Taha, H. (1997). Urban climates and heat islands: albedo, evapotranspiration, and anthropogenic heat. *Energy and Buildings*, *25*(2), 99–103. https://doi.org/https://doi.org/10.1016/S0378-7788(96)00999-1

Tang, A., & Kemp, L. (2021). A Fate Worse Than Warming? Stratospheric Aerosol Injection and Global Catastrophic Risk. *Frontiers in Climate*, *3*. https://doi.org/10.3389/FCLIM.2021.720312/FULL

Thailand: Fighting floods with "sponge cities" | PreventionWeb. (n.d.). Retrieved June 7, 2024, from https://www.preventionweb.net/news/thailand-fighting-floods-sponge-cities

UMEP Manual — UMEP Manual documentation. (n.d.). Retrieved June 4, 2024, from https://umep-docs.readthedocs.io/en/latest/

Urban Cooling | The Natural Capital Project. (n.d.). Retrieved June 3, 2024, from https://naturalcapitalproject.stanford.edu/invest/urban-cooling

UrbanBEATS – A Planning-Support System for Blue Green Cities. (n.d.). Retrieved June 4, 2024, from https://urbanbeatsmodel.com/

Vieira, S. M., Kaymak, U., & Sousa, J. M. C. (2010). Cohen's kappa coefficient as a performance measure for feature selection. *International Conference on Fuzzy Systems*, 1–8. https://doi.org/10.1109/FUZZY.2010.5584447

Wang, Y., Ouyang, W., & Zhang, J. (2024). Matching supply and demand of cooling service provided by urban green and blue space. *Urban Forestry & Urban Greening*, *96*, 128338. https://doi.org/https://doi.org/10.1016/j.ufug.2024.128338

Welcome to Lahore | Lahore. (n.d.). Retrieved June 6, 2024, from https://lahore.punjab.gov.pk/

Yin, Y., He, L., Wennberg, P. O., & Frankenberg, C. (2024). Unequal exposure to heatwaves in Los Angeles: Impact of uneven green spaces. *Science Advances*, *9*(17), eade8501. https://doi.org/10.1126/sciadv.ade8501

Zardo, L., Geneletti, D., Pérez-Soba, M., & Van Eupen, M. (2017). Estimating the cooling capacity of green infrastructures to support urban planning. *Ecosystem Services*, *26*, 225–235. https://doi.org/https://doi.org/10.1016/j.ecoser.2017.06.016

Zawadzka, J. E., Harris, J. A., & Corstanje, R. (2021a). Assessment of heat mitigation capacity of urban greenspaces with the use of InVEST urban cooling model, verified with day-time land surface temperature data. *Landscape and Urban Planning*, *214*. https://doi.org/10.1016/J.LANDURBPLAN.2021.104163

Zawadzka, J. E., Harris, J. A., & Corstanje, R. (2021b). Assessment of heat mitigation capacity of urban greenspaces with the use of InVEST urban cooling model, verified with day-time land surface temperature data. *Landscape and Urban Planning*, *214*. https://doi.org/10.1016/j.landurbplan.2021.104163

Zhang, N., Zhen, W., Shi, D., Zhong, C., & Li, Y. (2024). Quantification and mapping of the cooling effect of urban parks on the temperate monsoon climate zone. *Sustainable Cities and Society*, *101*, 105111. https://doi.org/https://doi.org/10.1016/j.scs.2023.105111

Zhang, W., Huang, B., & Luo, D. (2014). Effects of land use and transportation on carbon sources and carbon sinks: A case study in Shenzhen, China. *Landscape and Urban Planning*, *122*, 175–185. https://doi.org/10.1016/j.landurbplan.2013.09.014

Zhou, Y., Feng, Z., Xu, K., Wu, K., Gao, H., & Liu, P. (2023). Ecosystem Service Flow Perspective of Urban Green Land: Spatial Simulation and Driving Factors of Cooling Service Flow. *Land*, *12*(8). https://doi.org/10.3390/land12081527